Road Geometry Estimation Using Vehicle Trails: A Linear Mixed Model Approach

Yi-Chen Zhang
Sr. Engineer, Autonomous and Artificial Intelligence

Isuzu Technical Center of America

January 17, 2025

Outline

Outline

Motivation: Road geometry estimation

Road geometry

- the upcoming road geometry in front of the ego vehicle is of interest.
- received from the HD map or estimated from the on-board sensors.
- many of the features within ADAS technologies depend upon accurate information about it.
- the importance of the road geometry estimation accurately for ADAS systems has long been recognized:
  - crucial for the planning and control module;
  - development of planning strategies;
  - real-time route guidance in advanced navigation systems, among others.

Motivation: Road geometry estimation

Road geometry

- the upcoming road geometry in front of the ego vehicle is of interest.
- received from the HD map or estimated from the on-board sensors.
- many of the features within ADAS technologies depend upon accurate information about it.
- the importance of the road geometry estimation accurately for ADAS systems has long been recognized:
  - crucial for the planning and control module;
  - development of planning strategies;
  - real-time route guidance in advanced navigation systems, among others.

Motivation: Road geometry estimation

Road geometry

- the upcoming road geometry in front of the ego vehicle is of interest.
- received from the HD map or estimated from the on-board sensors.
- many of the features within ADAS technologies depend upon accurate information about it.
- the importance of the road geometry estimation accurately for ADAS systems has long been recognized:
  - crucial for the planning and control module;
  - development of planning strategies;
  - real-time route guidance in advanced navigation systems, among others.

Motivation: Road geometry estimation

Road geometry

- the upcoming road geometry in front of the ego vehicle is of interest.
- received from the HD map or estimated from the on-board sensors.
- many of the features within ADAS technologies depend upon accurate information about it.
- the importance of the road geometry estimation accurately for ADAS systems has long been recognized:
  - crucial for the planning and control module;
  - development of planning strategies;
  - real-time route guidance in advanced navigation systems, among others.

Motivation: Road geometry estimation

Road geometry

- the upcoming road geometry in front of the ego vehicle is of interest.
- received from the HD map or estimated from the on-board sensors.
- many of the features within ADAS technologies depend upon accurate information about it.
- the importance of the road geometry estimation accurately for ADAS systems has long been recognized:
  - crucial for the planning and control module;
  - development of planning strategies;
  - real-time route guidance in advanced navigation systems, among others.

Motivation: Road geometry estimation

Road geometry

- the upcoming road geometry in front of the ego vehicle is of interest.
- received from the HD map or estimated from the on-board sensors.
- many of the features within ADAS technologies depend upon accurate information about it.
- the importance of the road geometry estimation accurately for ADAS systems has long been recognized:
  - crucial for the planning and control module;
  - development of planning strategies;
  - real-time route guidance in advanced navigation systems, among others.

Motivation: Road geometry estimation

Road geometry

- the upcoming road geometry in front of the ego vehicle is of interest.
- received from the HD map or estimated from the on-board sensors.
- many of the features within ADAS technologies depend upon accurate information about it.
- the importance of the road geometry estimation accurately for ADAS systems has long been recognized:
  - crucial for the planning and control module;
  - development of planning strategies;
  - real-time route guidance in advanced navigation systems, among others.

Literature review: Road geometry estimation

Techniques of road geometry estimation has been investigated.

- Vision based: Chapuis et al. (2002); Wang et al. (2004, 2008); McCall & Trivedi (2006); Shin et al. (2014);
- Radar based: Yamaguchi et al. (1996); Kaliyaperumal et al. (2001); Wijesoma et al. (2004);
- Lidar based: Peterson et al. (2008); Yang et al. (2012); Quackenbush et al. (2003);
- Combined: Ma et al. (2000); Alessandretti et al. (2007); Lundquist et al. (2011); Garcìa-Fernàndez et al. (2014); Hammarstrand et al (2016);
- Included objects tracking: Eidehall et al. (2007); Garcìa-Fernàndez et al. (2014); Hammarstrand et al. (2016);
- Using trails of leading vehicles to estimate the road geometry?

Literature review: Road geometry estimation

Techniques of road geometry estimation has been investigated.

- Vision based: Chapuis et al. (2002); Wang et al. (2004, 2008); McCall & Trivedi (2006); Shin et al. (2014);
- Radar based: Yamaguchi et al. (1996); Kaliyaperumal et al. (2001); Wijesoma et al. (2004);
- Lidar based: Peterson et al. (2008); Yang et al. (2012); Quackenbush et al. (2003);
- Combined: Ma et al. (2000); Alessandretti et al. (2007); Lundquist et al. (2011); Garcìa-Fernàndez et al. (2014); Hammarstrand et al (2016);
- Included objects tracking: Eidehall et al. (2007); Garcìa-Fernàndez et al. (2014); Hammarstrand et al. (2016);
- Using trails of leading vehicles to estimate the road geometry?

Literature review: Road geometry estimation

Techniques of road geometry estimation has been investigated.

- Vision based: Chapuis et al. (2002); Wang et al. (2004, 2008); McCall & Trivedi (2006); Shin et al. (2014);
- Radar based: Yamaguchi et al. (1996); Kaliyaperumal et al. (2001); Wijesoma et al. (2004);
- Lidar based: Peterson et al. (2008); Yang et al. (2012); Quackenbush et al. (2003);
- Combined: Ma et al. (2000); Alessandretti et al. (2007); Lundquist et al. (2011); Garcìa-Fernàndez et al. (2014); Hammarstrand et al (2016);
- Included objects tracking: Eidehall et al. (2007); Garcìa-Fernàndez et al. (2014); Hammarstrand et al. (2016);
- Using trails of leading vehicles to estimate the road geometry?

Literature review: Road geometry estimation

Techniques of road geometry estimation has been investigated.

- Vision based: Chapuis et al. (2002); Wang et al. (2004, 2008); McCall & Trivedi (2006); Shin et al. (2014);
- Radar based: Yamaguchi et al. (1996); Kaliyaperumal et al. (2001); Wijesoma et al. (2004);
- Lidar based: Peterson et al. (2008); Yang et al. (2012); Quackenbush et al. (2003);
- Combined: Ma et al. (2000); Alessandretti et al. (2007); Lundquist et al. (2011); Garcìa-Fernàndez et al. (2014); Hammarstrand et al (2016);
- Included objects tracking: Eidehall et al. (2007); Garcìa-Fernàndez et al. (2014); Hammarstrand et al. (2016);
- Using trails of leading vehicles to estimate the road geometry?

Literature review: Road geometry estimation

Techniques of road geometry estimation has been investigated.

- Vision based: Chapuis et al. (2002); Wang et al. (2004, 2008); McCall & Trivedi (2006); Shin et al. (2014);
- Radar based: Yamaguchi et al. (1996); Kaliyaperumal et al. (2001); Wijesoma et al. (2004);
- Lidar based: Peterson et al. (2008); Yang et al. (2012); Quackenbush et al. (2003);
- Combined: Ma et al. (2000); Alessandretti et al. (2007); Lundquist et al. (2011); Garcìa-Fernàndez et al. (2014); Hammarstrand et al (2016);
- Included objects tracking: Eidehall et al. (2007); Garcìa-Fernàndez et al. (2014); Hammarstrand et al. (2016);
- Using trails of leading vehicles to estimate the road geometry?

Literature review: Road geometry estimation

Techniques of road geometry estimation has been investigated.

- Vision based: Chapuis et al. (2002); Wang et al. (2004, 2008); McCall & Trivedi (2006); Shin et al. (2014);
- Radar based: Yamaguchi et al. (1996); Kaliyaperumal et al. (2001); Wijesoma et al. (2004);
- Lidar based: Peterson et al. (2008); Yang et al. (2012); Quackenbush et al. (2003);
- Combined: Ma et al. (2000); Alessandretti et al. (2007); Lundquist et al. (2011); Garcìa-Fernàndez et al. (2014); Hammarstrand et al (2016);
- Included objects tracking: Eidehall et al. (2007); Garcìa-Fernàndez et al. (2014); Hammarstrand et al. (2016);
- Using trails of leading vehicles to estimate the road geometry?

Literature review: Road geometry estimation

Techniques of road geometry estimation has been investigated.

- Vision based: Chapuis et al. (2002); Wang et al. (2004, 2008); McCall & Trivedi (2006); Shin et al. (2014);
- Radar based: Yamaguchi et al. (1996); Kaliyaperumal et al. (2001); Wijesoma et al. (2004);
- Lidar based: Peterson et al. (2008); Yang et al. (2012); Quackenbush et al. (2003);
- Combined: Ma et al. (2000); Alessandretti et al. (2007); Lundquist et al. (2011); Garcìa-Fernàndez et al. (2014); Hammarstrand et al (2016);
- Included objects tracking: Eidehall et al. (2007); Garcìa-Fernàndez et al. (2014); Hammarstrand et al. (2016);
- Using trails of leading vehicles to estimate the road geometry?

Next generation simulation (NGSIM) data

- Overlook of the highway vehicle trajectory data.

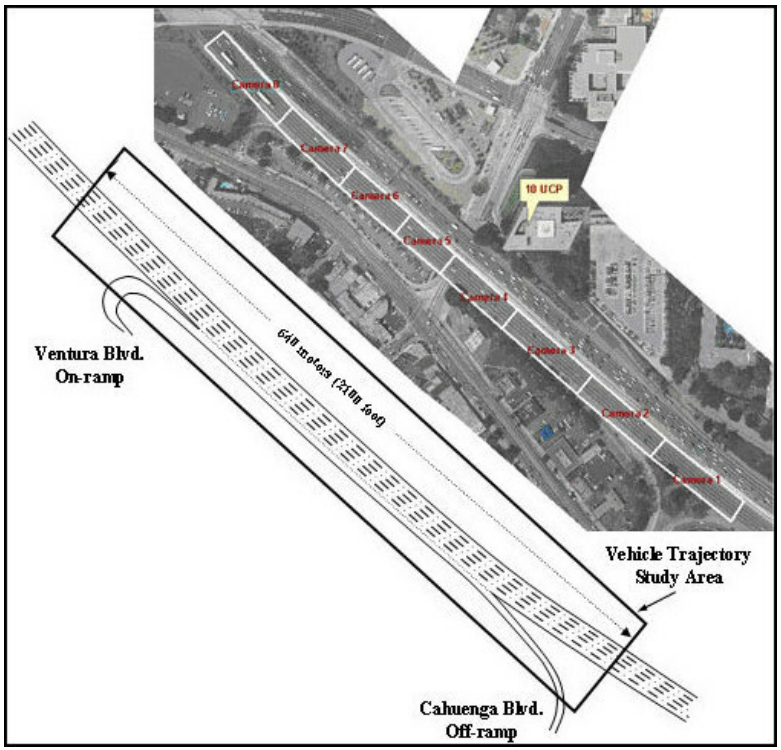

- The NGSIM data were originally collected by digital video cameras mounted on top of buildings located at US-101 and I-80 freeways in California.
- The sampling frequency of the NGSIM trajectories is 10 Hz.

Next generation simulation (NGSIM) data

- Overlook of the highway vehicle trajectory data.

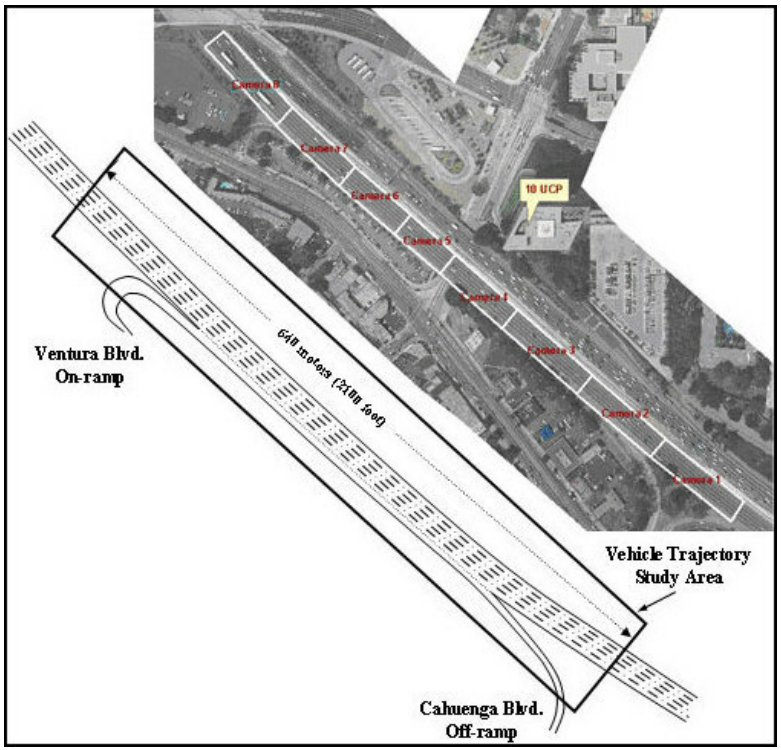

- The NGSIM data were originally collected by digital video cameras mounted on top of buildings located at US-101 and I-80 freeways in California.
- The sampling frequency of the NGSIM trajectories is 10 Hz.

Next generation simulation (NGSIM) data

- Overlook of the highway vehicle trajectory data.

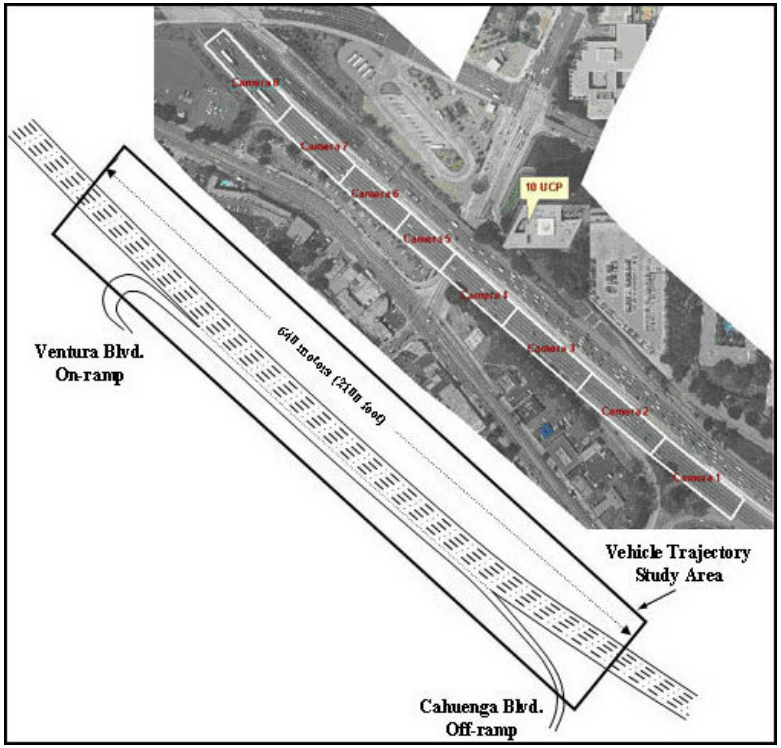

- The NGSIM data were originally collected by digital video cameras mounted on top of buildings located at US-101 and I-80 freeways in California.
- The sampling frequency of the NGSIM trajectories is 10 Hz.

- The NGSIM datasets were extracted from the resulting video images.

Vehicle_ID	Frame_ID	Total_Frames	Global_Time	Local_X	Local_Y	Global_X	Global_Y	v_length	v_Width	v_Class	v_Vel	v_Acc
352	3380	1156	1163368300	-5.359	0	2230502.921	1375532.938	15	6.5	2	33.96	0
352	3379	1156	1163368200	-4.623	4.566	2230503.114	1375537.934	15	6.5	2	33.96	0
352	3378	1156	1163368100	-4.707	7.606	2230502.731	1375540.951	15	6.5	2	33.96	0
39	208	1598	1163051100	11.573	12.311	2230518.568	1375546.762	15	7	2	0.25	-4.89
39	217	1598	1163052000	11.577	12.349	2230518.568	1375546.768	15	7	2	0.94	8.66
39	216	1598	1163051900	11.574	12.326	2230518.568	1375546.769	15	7	2	0.29	4.36

Lane_ID	O_Zone	D_Zone	Int_ID	Section_ID	Direction	Movement	Preceding	Following	Space_Headway	Time_Headway	Location
1	121	201	0	1	4	1	0	455	0	0	US-101
1	121	201	0	1	4	1	0	455	0	0	US-101
1	121	201	0	1	4	1	0	455	0	0	US-101
1	101	214	0	1	2	1	17	0	28.27	113.1	US-101
1	101	214	0	1	2	1	17	0	30.18	32.11	US-101
1	101	214	0	1	2	1	17	0	29.81	102.8	US-101

- The NGSIM datasets were extracted from the resulting video images.

Vehicle_ID	Frame_ID	Total_Frames	Global_Time	Local_X	Local_Y	Global_X	Global_Y	v_length	v_Width	v_Class	v_Vel	v_Acc
352	3380	1156	1163368300	-5.359	0	2230502.921	1375532.938	15	6.5	2	33.96	0
352	3379	1156	1163368200	-4.623	4.566	2230503.114	1375537.934	15	6.5	2	33.96	0
352	3378	1156	1163368100	-4.707	7.606	2230502.731	1375540.951	15	6.5	2	33.96	0
39	208	1598	1163051100	11.573	12.311	2230518.568	1375546.762	15	7	2	0.25	-4.89
39	217	1598	1163052000	11.577	12.349	2230518.568	1375546.768	15	7	2	0.94	8.66
39	216	1598	1163051900	11.574	12.326	2230518.568	1375546.769	15	7	2	0.29	4.36

Lane_ID	O_Zone	D_Zone	Int_ID	Section_ID	Direction	Movement	Preceding	Following	Space_Headway	Time_Headway	Location
1	121	201	0	1	4	1	0	455	0	0	US-101
1	121	201	0	1	4	1	0	455	0	0	US-101
1	121	201	0	1	4	1	0	455	0	0	US-101
1	101	214	0	1	2	1	17	0	28.27	113.1	US-101
1	101	214	0	1	2	1	17	0	30.18	32.11	US-101
1	101	214	0	1	2	1	17	0	29.81	102.8	US-101

- We process the NGSIM datasets and use the raster images for vehicles as illustration.

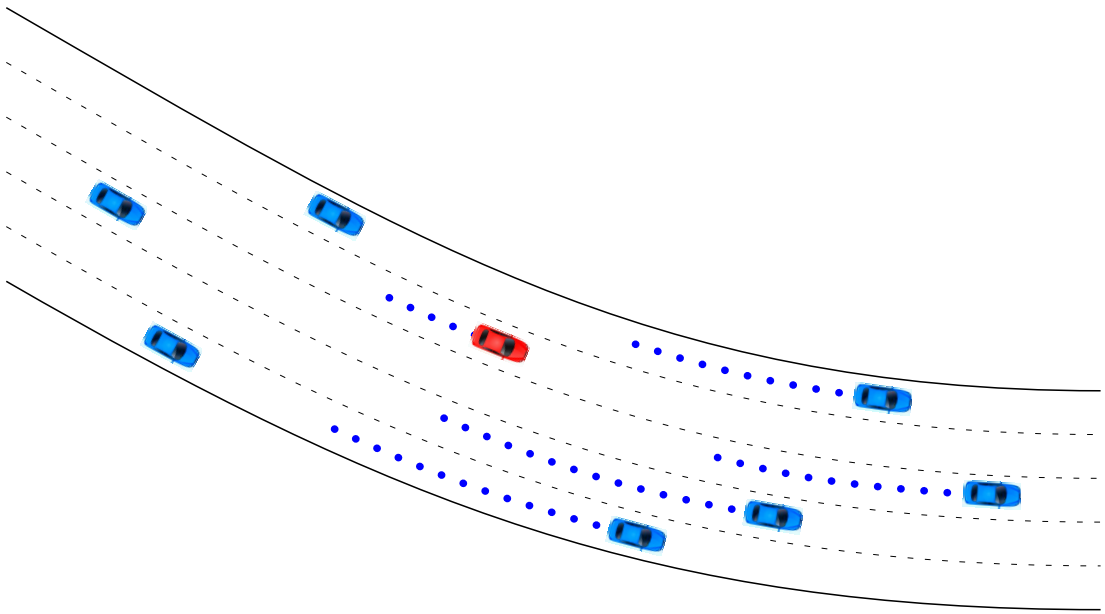

Road geometry definition and coordinate system

- The geometry of the road is defined as the shape that is parallel to the left and right road edges on a single road.
- We do not restrict the road shape to the middle of the host vehicle's lane.
- We use the third degree polynomial in which the lateral position is treated as a function of longitudinal position to describe the shape of the road.

Road geometry definition and coordinate system

- The geometry of the road is defined as the shape that is parallel to the left and right road edges on a single road.
- We do not restrict the road shape to the middle of the host vehicle's lane.
- We use the third degree polynomial in which the lateral position is treated as a function of longitudinal position to describe the shape of the road.

Road geometry definition and coordinate system

- The geometry of the road is defined as the shape that is parallel to the left and right road edges on a single road.
- We do not restrict the road shape to the middle of the host vehicle's lane.
- We use the third degree polynomial in which the lateral position is treated as a function of longitudinal position to describe the shape of the road.

Road geometry definition and coordinate system

- The geometry of the road is defined as the shape that is parallel to the left and right road edges on a single road.
- We do not restrict the road shape to the middle of the host vehicle's lane.
- We use the third degree polynomial in which the lateral position is treated as a function of longitudinal position to describe the shape of the road.
- Illustration of the estimated road shape (in yellow) and the true road shape (in purple).
- We call this mean trajectory dominated by trails the dominant road shape (DRS).

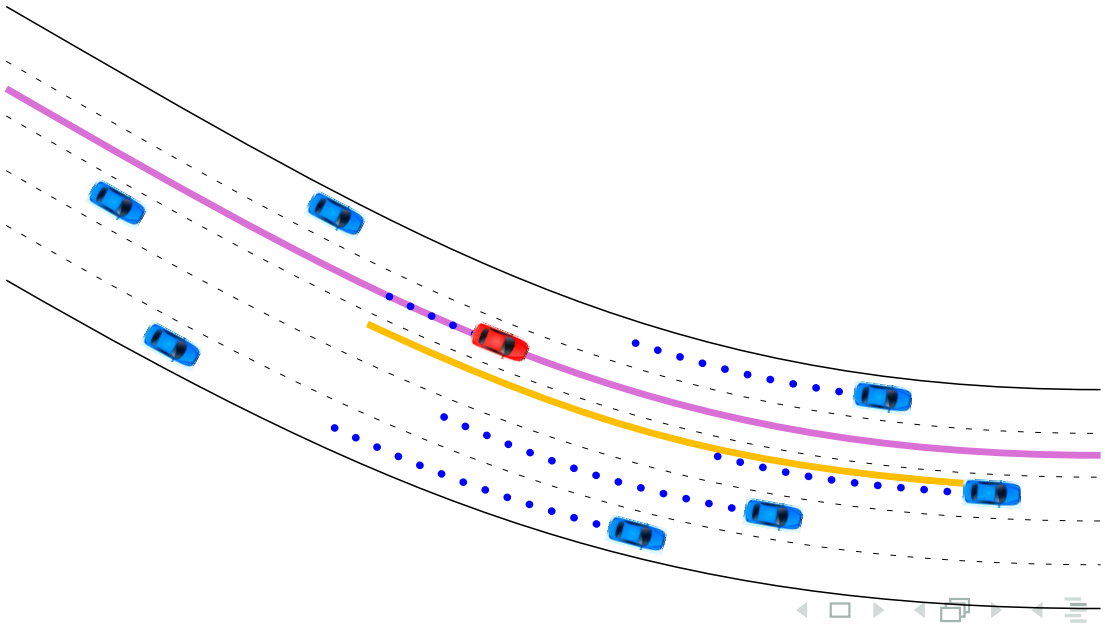

- We use a stationary frame of reference where the local coordinate system $[x^{l_k}, y^{l_k}]$ follows the ISO-8855 standard and is attached to the host vehicle.
- The subscript k refers to a time instance t_k and the superscript l_k is referring to the local coordinate system at time t_k.
- This local coordinate frame moves with the host vehicle and the measurement in this local coordinate frame is denoted as $(x_k^{l_k}, y_k^{l_k})^T$.
- The position and the orientation of the host vehicle in this local coordinate frame is expressed in the fixed global Cartesian coordinate system $[x^g, y^g]$ as $(x_{hk}^g, y_{hk}^g)^T$, and ϕ_{hk}^g, respectively.

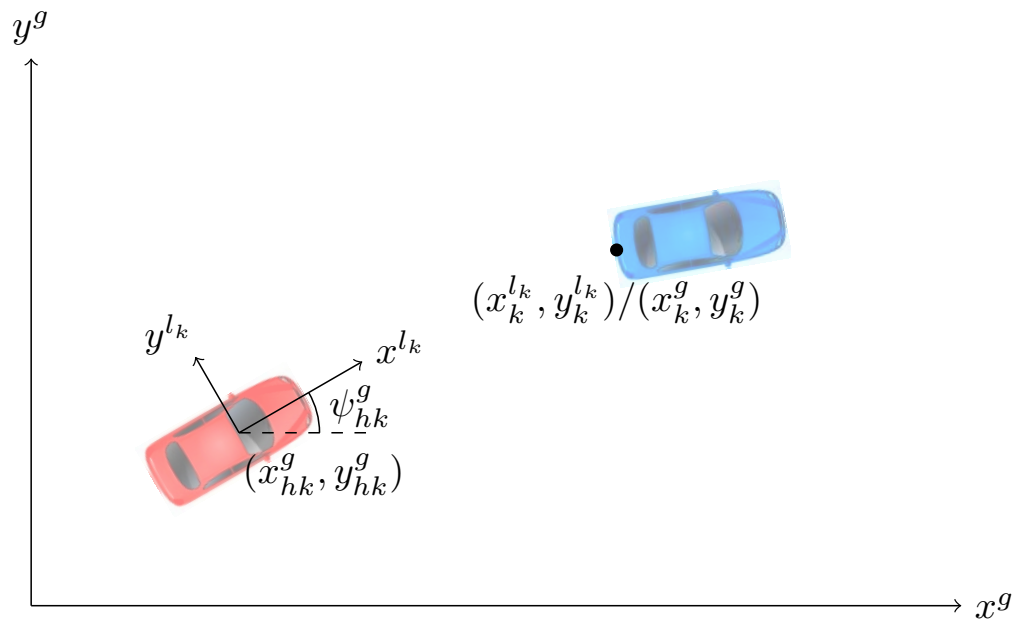

- We use a stationary frame of reference where the local coordinate system $[x^{l_k}, y^{l_k}]$ follows the ISO-8855 standard and is attached to the host vehicle.
- The subscript k refers to a time instance t_k and the superscript l_k is referring to the local coordinate system at time t_k.
- This local coordinate frame moves with the host vehicle and the measurement in this local coordinate frame is denoted as $(x_k^{l_k}, y_k^{l_k})^T$.
- The position and the orientation of the host vehicle in this local coordinate frame is expressed in the fixed global Cartesian coordinate system $[x^g, y^g]$ as $(x_{hk}^g, y_{hk}^g)^T$, and ϕ_{hk}^g, respectively.

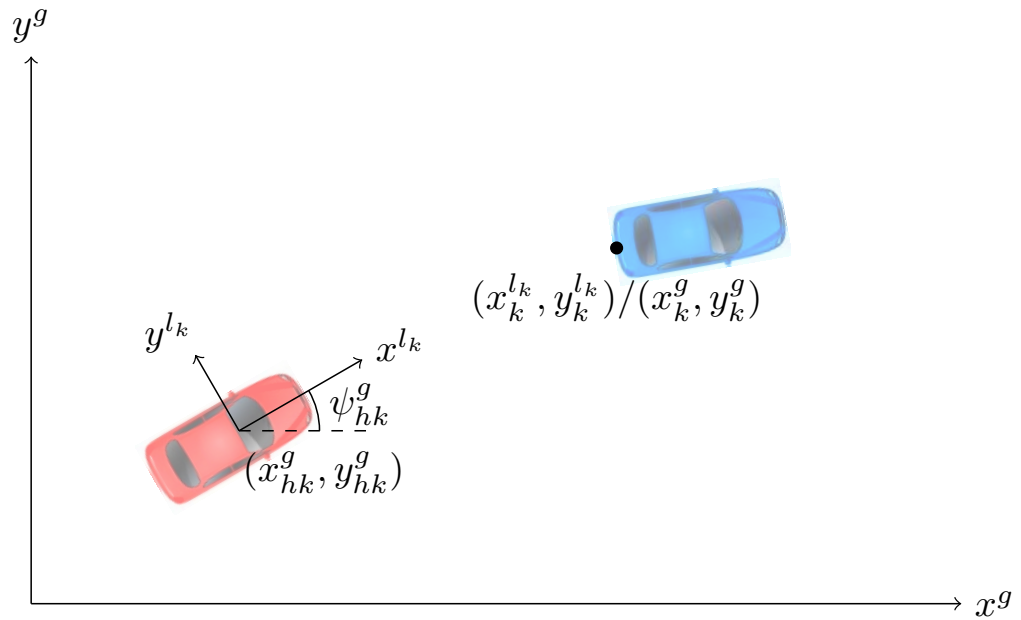

- We use a stationary frame of reference where the local coordinate system $[x^{l_k}, y^{l_k}]$ follows the ISO-8855 standard and is attached to the host vehicle.
- The subscript k refers to a time instance t_k and the superscript l_k is referring to the local coordinate system at time t_k.
- This local coordinate frame moves with the host vehicle and the measurement in this local coordinate frame is denoted as $(x_k^{l_k}, y_k^{l_k})^T$.
- The position and the orientation of the host vehicle in this local coordinate frame is expressed in the fixed global Cartesian coordinate system $[x^g, y^g]$ as $(x_{hk}^g, y_{hk}^g)^T$, and ϕ_{hk}^g, respectively.

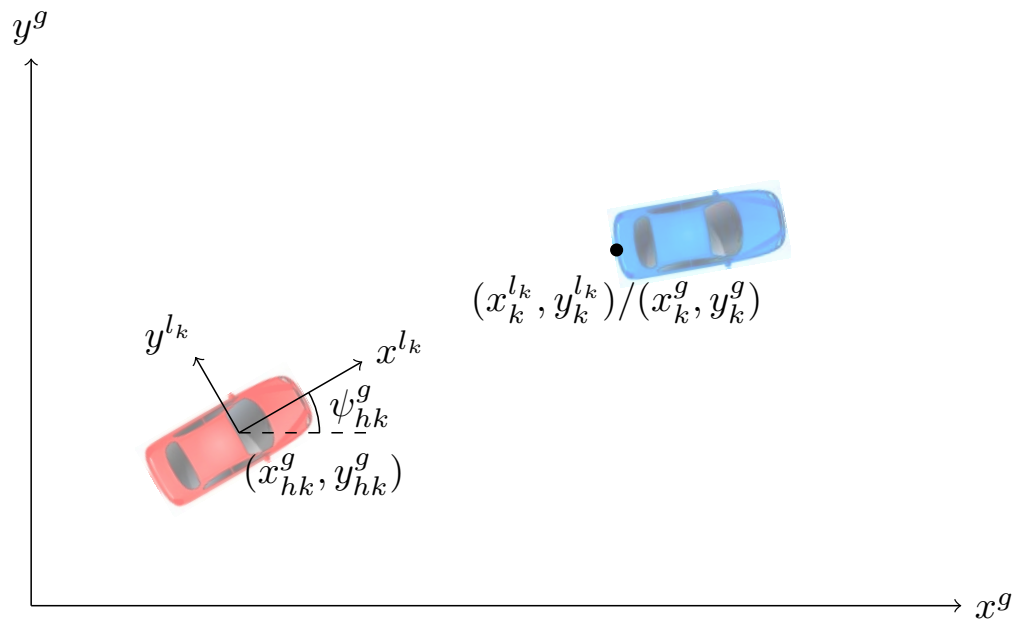

- We use a stationary frame of reference where the local coordinate system $[x^{l_k}, y^{l_k}]$ follows the ISO-8855 standard and is attached to the host vehicle.
- The subscript k refers to a time instance t_k and the superscript l_k is referring to the local coordinate system at time t_k.
- This local coordinate frame moves with the host vehicle and the measurement in this local coordinate frame is denoted as $(x_k^{l_k}, y_k^{l_k})^T$.
- The position and the orientation of the host vehicle in this local coordinate frame is expressed in the fixed global Cartesian coordinate system $[x^g, y^g]$ as $(x_{hk}^g, y_{hk}^g)^T$, and ϕ_{hk}^g, respectively.

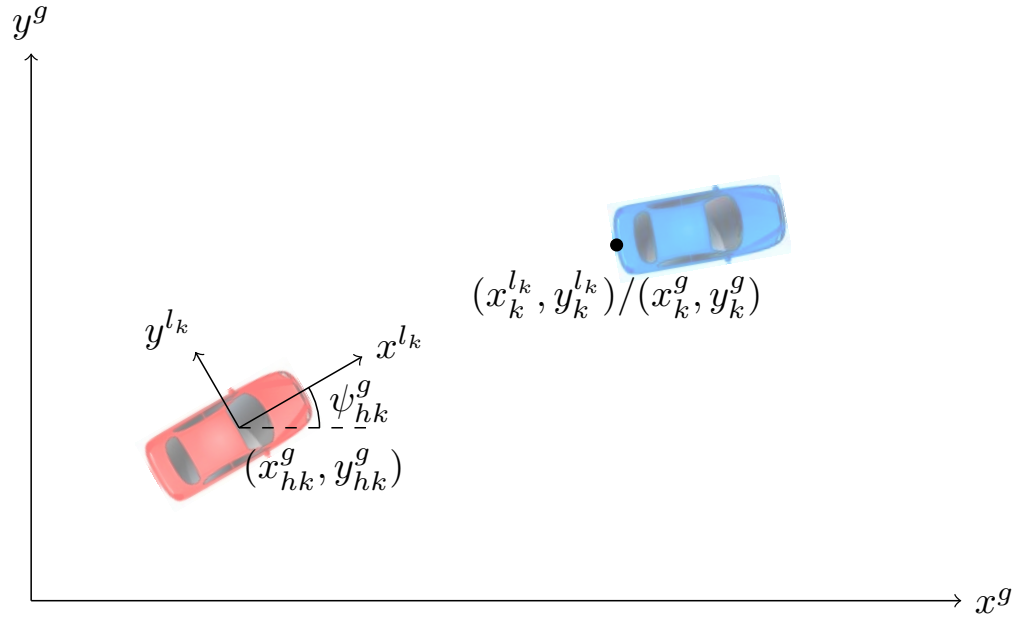

- There exists a non-linear transformation from the global coordinate frame to the local coordinate frame.
- The measurement $(x_k^g, y_k^g)^T$ is transformed to $(x_k^{l_k}, y_k^{l_k})^T$ using

$$\begin{pmatrix} x_k^{l_k} \\ y_k^{l_k} \end{pmatrix} = \begin{pmatrix} \cos\psi_{hk}^g & \sin\psi_{hk}^g \\ -\sin\psi_{hk}^g & \cos\psi_{hk}^g \end{pmatrix} \left(\begin{pmatrix} x_k^g \\ y_k^g \end{pmatrix} - \begin{pmatrix} x_{hk}^g \\ y_{hk}^g \end{pmatrix} \right) \tag{1}$$

- We assume that both the position $(x_{hk}^g, y_{hk}^g)^T$ and the orientation ψ_{hk}^g of the host vehicle are known for any time instance t_k.
- The inverse transformation can be calculated in a similar way using

$$\begin{pmatrix} x_k^g \\ y_k^g \end{pmatrix} = \begin{pmatrix} \cos\psi_{hk}^g & -\sin\psi_{hk}^g \\ \sin\psi_{hk}^g & \cos\psi_{hk}^g \end{pmatrix} \begin{pmatrix} x_k^{l_k} \\ y_k^{l_k} \end{pmatrix} + \begin{pmatrix} x_{hk}^g \\ y_{hk}^g \end{pmatrix}, \tag{2}$$

- There exists a non-linear transformation from the global coordinate frame to the local coordinate frame.
- The measurement $(x_k^g, y_k^g)^T$ is transformed to $(x_k^{l_k}, y_k^{l_k})^T$ using

$$\begin{pmatrix} x_k^{l_k} \\ y_k^{l_k} \end{pmatrix} = \begin{pmatrix} \cos\psi_{hk}^g & \sin\psi_{hk}^g \\ -\sin\psi_{hk}^g & \cos\psi_{hk}^g \end{pmatrix} \left(\begin{pmatrix} x_k^g \\ y_k^g \end{pmatrix} - \begin{pmatrix} x_{hk}^g \\ y_{hk}^g \end{pmatrix} \right) \tag{1}$$

- We assume that both the position $(x_{hk}^g, y_{hk}^g)^T$ and the orientation ψ_{hk}^g of the host vehicle are known for any time instance t_k.
- The inverse transformation can be calculated in a similar way using

$$\begin{pmatrix} x_k^g \\ y_k^g \end{pmatrix} = \begin{pmatrix} \cos\psi_{hk}^g & -\sin\psi_{hk}^g \\ \sin\psi_{hk}^g & \cos\psi_{hk}^g \end{pmatrix} \begin{pmatrix} x_k^{l_k} \\ y_k^{l_k} \end{pmatrix} + \begin{pmatrix} x_{hk}^g \\ y_{hk}^g \end{pmatrix}, \tag{2}$$

- There exists a non-linear transformation from the global coordinate frame to the local coordinate frame.
- The measurement $(x_k^g, y_k^g)^T$ is transformed to $(x_k^{l_k}, y_k^{l_k})^T$ using

$$\begin{pmatrix} x_k^{l_k} \\ y_k^{l_k} \end{pmatrix} = \begin{pmatrix} \cos\psi_{hk}^g & \sin\psi_{hk}^g \\ -\sin\psi_{hk}^g & \cos\psi_{hk}^g \end{pmatrix} \left(\begin{pmatrix} x_k^g \\ y_k^g \end{pmatrix} - \begin{pmatrix} x_{hk}^g \\ y_{hk}^g \end{pmatrix} \right) \tag{1}$$

- We assume that both the position $(x_{hk}^g, y_{hk}^g)^T$ and the orientation ψ_{hk}^g of the host vehicle are known for any time instance t_k.
- The inverse transformation can be calculated in a similar way using

$$\begin{pmatrix} x_k^g \\ y_k^g \end{pmatrix} = \begin{pmatrix} \cos\psi_{hk}^g & -\sin\psi_{hk}^g \\ \sin\psi_{hk}^g & \cos\psi_{hk}^g \end{pmatrix} \begin{pmatrix} x_k^{l_k} \\ y_k^{l_k} \end{pmatrix} + \begin{pmatrix} x_{hk}^g \\ y_{hk}^g \end{pmatrix}, \tag{2}$$

- There exists a non-linear transformation from the global coordinate frame to the local coordinate frame.
- The measurement $(x_k^g, y_k^g)^T$ is transformed to $(x_k^{l_k}, y_k^{l_k})^T$ using

$$\begin{pmatrix} x_k^{l_k} \\ y_k^{l_k} \end{pmatrix} = \begin{pmatrix} \cos\psi_{hk}^g & \sin\psi_{hk}^g \\ -\sin\psi_{hk}^g & \cos\psi_{hk}^g \end{pmatrix} \left(\begin{pmatrix} x_k^g \\ y_k^g \end{pmatrix} - \begin{pmatrix} x_{hk}^g \\ y_{hk}^g \end{pmatrix} \right) \tag{1}$$

- We assume that both the position $(x_{hk}^g, y_{hk}^g)^T$ and the orientation ψ_{hk}^g of the host vehicle are known for any time instance t_k.
- The inverse transformation can be calculated in a similar way using

$$\begin{pmatrix} x_k^g \\ y_k^g \end{pmatrix} = \begin{pmatrix} \cos\psi_{hk}^g & -\sin\psi_{hk}^g \\ \sin\psi_{hk}^g & \cos\psi_{hk}^g \end{pmatrix} \begin{pmatrix} x_k^{l_k} \\ y_k^{l_k} \end{pmatrix} + \begin{pmatrix} x_{hk}^g \\ y_{hk}^g \end{pmatrix}, \tag{2}$$

Observations and vehicle trails

- Suppose the host vehicle has tracked the i-th leading vehicle from time t_j to time t_l. For each time instance t_k, with $j \leq k \leq l$, the reference point of guest vehicle $(x_{ik}^{l_k}, y_{ik}^{l_k})^T$ is then converted into $(x_{ik}^{g}, y_{ik}^{g})^T$.
- The collection of all pairs $\{(x_{ik}^{g}, y_{ik}^{g})^T\}_{j \leq k \leq l}$ forms the samples from i-th vehicle's trail. Any newly observed measurements of the i-th vehicle are appended to the i-th vehicle's trail in the same manner.
- The size of trail samples grows extremely rapidly. To keep the trail sample size under control and also to preserve the shape of the trail, we introduce trail compression and chopping mechanisms to address this issue.
- Trail compression: Squeezes samples of trails that do not contribute to the fundamental road geometry. This naturally gets us the behavior where we keep more samples through curves and fewer samples through straightaways.
- Trail chopping: Removes trail samples that are obsolete. With the host vehicle moving forward, the trail samples behind are not useful anymore for upcoming road geometry

Observations and vehicle trails

- Suppose the host vehicle has tracked the i-th leading vehicle from time t_j to time t_l. For each time instance t_k, with $j \leq k \leq l$, the reference point of guest vehicle $(x_{ik}^{l_k}, y_{ik}^{l_k})^T$ is then converted into $(x_{ik}^{g}, y_{ik}^{g})^T$.
- The collection of all pairs $\{(x_{ik}^{g}, y_{ik}^{g})^T\}_{j \leq k \leq l}$ forms the samples from i-th vehicle's trail. Any newly observed measurements of the i-th vehicle are appended to the i-th vehicle's trail in the same manner.
- The size of trail samples grows extremely rapidly. To keep the trail sample size under control and also to preserve the shape of the trail, we introduce trail compression and chopping mechanisms to address this issue.
- Trail compression: Squeezes samples of trails that do not contribute to the fundamental road geometry. This naturally gets us the behavior where we keep more samples through curves and fewer samples through straightaways.
- Trail chopping: Removes trail samples that are obsolete. With the host vehicle moving forward, the trail samples behind are not useful anymore for upcoming road geometry

Observations and vehicle trails

- Suppose the host vehicle has tracked the i-th leading vehicle from time t_j to time t_l. For each time instance t_k, with $j \leq k \leq l$, the reference point of guest vehicle $(x_{ik}^{l_k}, y_{ik}^{l_k})^T$ is then converted into $(x_{ik}^{g}, y_{ik}^{g})^T$.
- The collection of all pairs $\{(x_{ik}^{g}, y_{ik}^{g})^T\}_{j \leq k \leq l}$ forms the samples from i-th vehicle's trail. Any newly observed measurements of the i-th vehicle are appended to the i-th vehicle's trail in the same manner.
- The size of trail samples grows extremely rapidly. To keep the trail sample size under control and also to preserve the shape of the trail, we introduce trail compression and chopping mechanisms to address this issue.
- Trail compression: Squeezes samples of trails that do not contribute to the fundamental road geometry. This naturally gets us the behavior where we keep more samples through curves and fewer samples through straightaways.
- Trail chopping: Removes trail samples that are obsolete. With the host vehicle moving forward, the trail samples behind are not useful anymore for upcoming road geometry

Observations and vehicle trails

- Suppose the host vehicle has tracked the i-th leading vehicle from time t_j to time t_l. For each time instance t_k, with $j \leq k \leq l$, the reference point of guest vehicle $(x_{ik}^{l_k}, y_{ik}^{l_k})^T$ is then converted into $(x_{ik}^{g}, y_{ik}^{g})^T$.
- The collection of all pairs $\{(x_{ik}^{g}, y_{ik}^{g})^T\}_{j \leq k \leq l}$ forms the samples from i-th vehicle's trail. Any newly observed measurements of the i-th vehicle are appended to the i-th vehicle's trail in the same manner.
- The size of trail samples grows extremely rapidly. To keep the trail sample size under control and also to preserve the shape of the trail, we introduce trail compression and chopping mechanisms to address this issue.
- Trail compression: Squeezes samples of trails that do not contribute to the fundamental road geometry. This naturally gets us the behavior where we keep more samples through curves and fewer samples through straightaways.
- Trail chopping: Removes trail samples that are obsolete. With the host vehicle moving forward, the trail samples behind are not useful anymore for upcoming road geometry

Observations and vehicle trails

- Suppose the host vehicle has tracked the i-th leading vehicle from time t_j to time t_l. For each time instance t_k, with $j \leq k \leq l$, the reference point of guest vehicle $(x_{ik}^{l_k}, y_{ik}^{l_k})^T$ is then converted into $(x_{ik}^{g}, y_{ik}^{g})^T$.
- The collection of all pairs $\{(x_{ik}^{g}, y_{ik}^{g})^T\}_{j \leq k \leq l}$ forms the samples from i-th vehicle's trail. Any newly observed measurements of the i-th vehicle are appended to the i-th vehicle's trail in the same manner.
- The size of trail samples grows extremely rapidly. To keep the trail sample size under control and also to preserve the shape of the trail, we introduce trail compression and chopping mechanisms to address this issue.
- Trail compression: Squeezes samples of trails that do not contribute to the fundamental road geometry. This naturally gets us the behavior where we keep more samples through curves and fewer samples through straightaways.
- Trail chopping: Removes trail samples that are obsolete. With the host vehicle moving forward, the trail samples behind are not useful anymore for upcoming road geometry

Outline

Modeling the road shape using vehicle trails

- The real road shape is designed to be smooth enough for safe driving.
- We assume the road shape is a smooth function in which the lateral position is related to the longitudinal position in the local coordinate frame:

$$y = \mu(x), \tag{3}$$

- We work in the local coordinate frame and assume that the DRS can be modeled by a third-degree polynomial

$$y = \beta_0 + \beta_1 x + \beta_2 x^2 + \beta_3 x^3, \tag{4}$$

  where $\boldsymbol{\beta} = (\beta_0, \ldots, \beta_3)^T$ are unknown coefficients.
- The aim is to estimate the unknown coefficients $\boldsymbol{\beta}$ such that the DRS presented in (4) can be used to delineate the road shape μ in (3).

Modeling the road shape using vehicle trails

- The real road shape is designed to be smooth enough for safe driving.
- We assume the road shape is a smooth function in which the lateral position is related to the longitudinal position in the local coordinate frame:

$$y = \mu(x), \tag{3}$$

- We work in the local coordinate frame and assume that the DRS can be modeled by a third-degree polynomial

$$y = \beta_0 + \beta_1 x + \beta_2 x^2 + \beta_3 x^3, \tag{4}$$

  where $\boldsymbol{\beta} = (\beta_0, \ldots, \beta_3)^T$ are unknown coefficients.
- The aim is to estimate the unknown coefficients $\boldsymbol{\beta}$ such that the DRS presented in (4) can be used to delineate the road shape μ in (3).

Modeling the road shape using vehicle trails

- The real road shape is designed to be smooth enough for safe driving.
- We assume the road shape is a smooth function in which the lateral position is related to the longitudinal position in the local coordinate frame:

$$y = \mu(x), \tag{3}$$

- We work in the local coordinate frame and assume that the DRS can be modeled by a third-degree polynomial

$$y = \beta_0 + \beta_1 x + \beta_2 x^2 + \beta_3 x^3, \tag{4}$$

  where $\boldsymbol{\beta} = (\beta_0, \ldots, \beta_3)^T$ are unknown coefficients.
- The aim is to estimate the unknown coefficients $\boldsymbol{\beta}$ such that the DRS presented in (4) can be used to delineate the road shape μ in (3).

Modeling the road shape using vehicle trails

- The real road shape is designed to be smooth enough for safe driving.
- We assume the road shape is a smooth function in which the lateral position is related to the longitudinal position in the local coordinate frame:

$$y = \mu(x), \tag{3}$$

- We work in the local coordinate frame and assume that the DRS can be modeled by a third-degree polynomial

$$y = \beta_0 + \beta_1 x + \beta_2 x^2 + \beta_3 x^3, \tag{4}$$

  where $\boldsymbol{\beta} = (\beta_0, \ldots, \beta_3)^T$ are unknown coefficients.
- The aim is to estimate the unknown coefficients $\boldsymbol{\beta}$ such that the DRS presented in (4) can be used to delineate the road shape μ in (3).

Linear mixed model (LMM) for trail samples

- The LMM algorithm is running at each time t_k. Note that the following notations are at time t_k without specifying the time step k.
- m is the number of leading vehicles
- n_i is the number of trail samples of the i-th vehicle, $i = 1, \ldots, m$. $n = \sum_{i=1}^{m} n_i$ is the trail sample in total.
- $x_{ij}^{l_k}$ is the j-th longitudinal position of the trail sample of i-th vehicle.
- $y_{ij}^{l_k}$ is the j-th lateral position of the trail sample of i-th vehicle, $j = 1, \ldots, n_i$.
- α_i is the lateral offset of the vehicle to the DRS.
- ϵ_{ij} is the measurement error.

Linear mixed model (LMM) for trail samples

- The LMM algorithm is running at each time t_k. Note that the following notations are at time t_k without specifying the time step k.
- m is the number of leading vehicles
- n_i is the number of trail samples of the i-th vehicle, $i = 1, \ldots, m$. $n = \sum_{i=1}^{m} n_i$ is the trail sample in total.
- $x_{ij}^{l_k}$ is the j-th longitudinal position of the trail sample of i-th vehicle.
- $y_{ij}^{l_k}$ is the j-th lateral position of the trail sample of i-th vehicle, $j = 1, \ldots, n_i$.
- α_i is the lateral offset of the vehicle to the DRS.
- ϵ_{ij} is the measurement error.

Linear mixed model (LMM) for trail samples

- The LMM algorithm is running at each time t_k. Note that the following notations are at time t_k without specifying the time step k.
- m is the number of leading vehicles
- n_i is the number of trail samples of the i-th vehicle, $i = 1, \ldots, m$. $n = \sum_{i=1}^{m} n_i$ is the trail sample in total.
- $x_{ij}^{l_k}$ is the j-th longitudinal position of the trail sample of i-th vehicle.
- $y_{ij}^{l_k}$ is the j-th lateral position of the trail sample of i-th vehicle, $j = 1, \ldots, n_i$.
- α_i is the lateral offset of the vehicle to the DRS.
- ϵ_{ij} is the measurement error.

Linear mixed model (LMM) for trail samples

- The LMM algorithm is running at each time t_k. Note that the following notations are at time t_k without specifying the time step k.
- m is the number of leading vehicles
- n_i is the number of trail samples of the i-th vehicle, $i = 1, \ldots, m$. $n = \sum_{i=1}^{m} n_i$ is the trail sample in total.
- $x_{ij}^{l_k}$ is the j-th longitudinal position of the trail sample of i-th vehicle.
- $y_{ij}^{l_k}$ is the j-th lateral position of the trail sample of i-th vehicle, $j = 1, \ldots, n_i$.
- α_i is the lateral offset of the vehicle to the DRS.
- ϵ_{ij} is the measurement error.

Linear mixed model (LMM) for trail samples

- The LMM algorithm is running at each time t_k. Note that the following notations are at time t_k without specifying the time step k.
- m is the number of leading vehicles
- n_i is the number of trail samples of the i-th vehicle, $i = 1, \ldots, m$. $n = \sum_{i=1}^{m} n_i$ is the trail sample in total.
- $x_{ij}^{l_k}$ is the j-th longitudinal position of the trail sample of i-th vehicle.
- $y_{ij}^{l_k}$ is the j-th lateral position of the trail sample of i-th vehicle, $j = 1, \ldots, n_i$.
- α_i is the lateral offset of the vehicle to the DRS.
- ϵ_{ij} is the measurement error.

Linear mixed model (LMM) for trail samples

- The LMM algorithm is running at each time t_k. Note that the following notations are at time t_k without specifying the time step k.
- m is the number of leading vehicles
- n_i is the number of trail samples of the i-th vehicle, $i = 1, \ldots, m$. $n = \sum_{i=1}^{m} n_i$ is the trail sample in total.
- $x_{ij}^{l_k}$ is the j-th longitudinal position of the trail sample of i-th vehicle.
- $y_{ij}^{l_k}$ is the j-th lateral position of the trail sample of i-th vehicle, $j = 1, \ldots, n_i$.
- α_i is the lateral offset of the vehicle to the DRS.
- ϵ_{ij} is the measurement error.

Linear mixed model (LMM) for trail samples

- The LMM algorithm is running at each time t_k. Note that the following notations are at time t_k without specifying the time step k.
- m is the number of leading vehicles
- n_i is the number of trail samples of the i-th vehicle, $i = 1, \ldots, m$. $n = \sum_{i=1}^{m} n_i$ is the trail sample in total.
- $x_{ij}^{l_k}$ is the j-th longitudinal position of the trail sample of i-th vehicle.
- $y_{ij}^{l_k}$ is the j-th lateral position of the trail sample of i-th vehicle, $j = 1, \ldots, n_i$.
- α_i is the lateral offset of the vehicle to the DRS.
- ϵ_{ij} is the measurement error.

- We assume that α_i has mean 0 and variance σ_α^2, and ϵ_{ij} has mean 0 and variance σ^2. Both of them are mutually independent.
- The model is

$$y_{ij}^{l_k} = \beta_0 + \beta_1 x_{ij}^{l_k} + \beta_2 (x_{ij}^{l_k})^2 + \beta_3 (x_{ij}^{l_k})^3 + \alpha_i + \epsilon_{ij}, \tag{5}$$

  for $i = 1, \ldots, m$ and $j = 1, \ldots, n_i$.
- The variance-covariance structure of $y_{ij}^{l_k}$ can be easily derived as

$$\text{Var}(y_{ij}^{l_k}) = \sigma_\alpha^2 + \sigma^2 \quad \text{and} \quad \text{Cov}(y_{ij}^{l_k}, y_{il}^{l_k}) = \sigma_\alpha^2 \text{ for } j \neq l.$$

- The σ_α^2 is the covariance between every pair of sample from the same vehicle.

- We assume that α_i has mean 0 and variance σ_α^2, and ϵ_{ij} has mean 0 and variance σ^2. Both of them are mutually independent.
- The model is

$$y_{ij}^{l_k} = \beta_0 + \beta_1 x_{ij}^{l_k} + \beta_2 (x_{ij}^{l_k})^2 + \beta_3 (x_{ij}^{l_k})^3 + \alpha_i + \epsilon_{ij}, \tag{5}$$

  for $i = 1, \ldots, m$ and $j = 1, \ldots, n_i$.
- The variance-covariance structure of $y_{ij}^{l_k}$ can be easily derived as

$$\text{Var}(y_{ij}^{l_k}) = \sigma_\alpha^2 + \sigma^2 \quad \text{and} \quad \text{Cov}(y_{ij}^{l_k}, y_{il}^{l_k}) = \sigma_\alpha^2 \text{ for } j \neq l.$$

- The σ_α^2 is the covariance between every pair of sample from the same vehicle.

- We assume that α_i has mean 0 and variance σ_α^2, and ϵ_{ij} has mean 0 and variance σ^2. Both of them are mutually independent.
- The model is

$$y_{ij}^{l_k} = \beta_0 + \beta_1 x_{ij}^{l_k} + \beta_2 (x_{ij}^{l_k})^2 + \beta_3 (x_{ij}^{l_k})^3 + \alpha_i + \epsilon_{ij}, \tag{5}$$

  for $i = 1, \ldots, m$ and $j = 1, \ldots, n_i$.
- The variance-covariance structure of $y_{ij}^{l_k}$ can be easily derived as

$$\text{Var}(y_{ij}^{l_k}) = \sigma_\alpha^2 + \sigma^2 \quad \text{and} \quad \text{Cov}(y_{ij}^{l_k}, y_{il}^{l_k}) = \sigma_\alpha^2 \text{ for } j \neq l.$$

- The σ_α^2 is the covariance between every pair of sample from the same vehicle.

- We assume that α_i has mean 0 and variance σ_α^2, and ϵ_{ij} has mean 0 and variance σ^2. Both of them are mutually independent.
- The model is

$$y_{ij}^{l_k} = \beta_0 + \beta_1 x_{ij}^{l_k} + \beta_2 (x_{ij}^{l_k})^2 + \beta_3 (x_{ij}^{l_k})^3 + \alpha_i + \epsilon_{ij}, \tag{5}$$

  for $i = 1, \ldots, m$ and $j = 1, \ldots, n_i$.
- The variance-covariance structure of $y_{ij}^{l_k}$ can be easily derived as

$$\text{Var}(y_{ij}^{l_k}) = \sigma_\alpha^2 + \sigma^2 \quad \text{and} \quad \text{Cov}(y_{ij}^{l_k}, y_{il}^{l_k}) = \sigma_\alpha^2 \text{ for } j \neq l.$$

- The σ_α^2 is the covariance between every pair of sample from the same vehicle.

- In matrix notation, the model can be rewrite as

$$\boldsymbol{y}_i = \boldsymbol{X}_i\boldsymbol{\beta} + \mathbf{1}_i\alpha_i + \boldsymbol{\epsilon}_i.$$

- $\mathrm{E}(\boldsymbol{y}_i) = \boldsymbol{X}_i\boldsymbol{\beta}$ and $\mathrm{Var}(\boldsymbol{y}_i) = \boldsymbol{V}_i$, where $\boldsymbol{V}_i = \sigma_\alpha^2 \mathbf{1}_{n_i}\mathbf{1}_{n_i}^T + \sigma^2 \boldsymbol{I}_{n_i}$.
- We then represent the vector of trail data for all vehicles:

$$\boldsymbol{y} = \boldsymbol{X}\boldsymbol{\beta} + \boldsymbol{Z}\boldsymbol{\alpha} + \boldsymbol{\epsilon}$$

  where $\boldsymbol{Z} = (\mathbf{1}_1, \ldots, \mathbf{1}_m)^T$.
- $\mathrm{E}(\boldsymbol{y}) = \boldsymbol{X}\boldsymbol{\beta}$ and $\mathrm{Var}(\boldsymbol{y}) = \boldsymbol{V}$, where $\boldsymbol{V} = \sigma_\alpha^2 \boldsymbol{Z}\boldsymbol{Z}^T + \sigma^2 \boldsymbol{I}$
- We can thus use the methodology that has been developed for LMMs in this context.

- In matrix notation, the model can be rewrite as

$$\boldsymbol{y}_i = \boldsymbol{X}_i\boldsymbol{\beta} + \mathbf{1}_i\alpha_i + \boldsymbol{\epsilon}_i.$$

- $\mathsf{E}(\boldsymbol{y}_i) = \boldsymbol{X}_i\boldsymbol{\beta}$ and $\mathsf{Var}(\boldsymbol{y}_i) = \boldsymbol{V}_i$, where $\boldsymbol{V}_i = \sigma_\alpha^2 \mathbf{1}_{n_i}\mathbf{1}_{n_i}^T + \sigma^2 \boldsymbol{I}_{n_i}$.
- We then represent the vector of trail data for all vehicles:

$$\boldsymbol{y} = \boldsymbol{X}\boldsymbol{\beta} + \boldsymbol{Z}\boldsymbol{\alpha} + \boldsymbol{\epsilon}$$

  where $\boldsymbol{Z} = (\mathbf{1}_1, \ldots, \mathbf{1}_m)^T$.
- $\mathsf{E}(\boldsymbol{y}) = \boldsymbol{X}\boldsymbol{\beta}$ and $\mathsf{Var}(\boldsymbol{y}) = \boldsymbol{V}$, where $\boldsymbol{V} = \sigma_\alpha^2 \boldsymbol{Z}\boldsymbol{Z}^T + \sigma^2 \boldsymbol{I}$
- We can thus use the methodology that has been developed for LMMs in this context.

- In matrix notation, the model can be rewrite as

$$\boldsymbol{y}_i = \boldsymbol{X}_i\boldsymbol{\beta} + \mathbf{1}_i\alpha_i + \boldsymbol{\epsilon}_i.$$

- $\mathrm{E}(\boldsymbol{y}_i) = \boldsymbol{X}_i\boldsymbol{\beta}$ and $\mathrm{Var}(\boldsymbol{y}_i) = \boldsymbol{V}_i$, where $\boldsymbol{V}_i = \sigma_\alpha^2 \mathbf{1}_{n_i}\mathbf{1}_{n_i}^T + \sigma^2 \boldsymbol{I}_{n_i}$.
- We then represent the vector of trail data for all vehicles:

$$\boldsymbol{y} = \boldsymbol{X}\boldsymbol{\beta} + \boldsymbol{Z}\boldsymbol{\alpha} + \boldsymbol{\epsilon}$$

  where $\boldsymbol{Z} = (\mathbf{1}_1, \ldots, \mathbf{1}_m)^T$.
- $\mathrm{E}(\boldsymbol{y}) = \boldsymbol{X}\boldsymbol{\beta}$ and $\mathrm{Var}(\boldsymbol{y}) = \boldsymbol{V}$, where $\boldsymbol{V} = \sigma_\alpha^2 \boldsymbol{Z}\boldsymbol{Z}^T + \sigma^2 \boldsymbol{I}$
- We can thus use the methodology that has been developed for LMMs in this context.

- In matrix notation, the model can be rewrite as

$$\boldsymbol{y}_i = \boldsymbol{X}_i\boldsymbol{\beta} + \mathbf{1}_i\alpha_i + \boldsymbol{\epsilon}_i.$$

- $\mathrm{E}(\boldsymbol{y}_i) = \boldsymbol{X}_i\boldsymbol{\beta}$ and $\mathrm{Var}(\boldsymbol{y}_i) = \boldsymbol{V}_i$, where $\boldsymbol{V}_i = \sigma_\alpha^2 \mathbf{1}_{n_i}\mathbf{1}_{n_i}^T + \sigma^2 \boldsymbol{I}_{n_i}$.
- We then represent the vector of trail data for all vehicles:

$$\boldsymbol{y} = \boldsymbol{X}\boldsymbol{\beta} + \boldsymbol{Z}\boldsymbol{\alpha} + \boldsymbol{\epsilon}$$

  where $\boldsymbol{Z} = (\mathbf{1}_1, \ldots, \mathbf{1}_m)^T$.
- $\mathrm{E}(\boldsymbol{y}) = \boldsymbol{X}\boldsymbol{\beta}$ and $\mathrm{Var}(\boldsymbol{y}) = \boldsymbol{V}$, where $\boldsymbol{V} = \sigma_\alpha^2 \boldsymbol{Z}\boldsymbol{Z}^T + \sigma^2 \boldsymbol{I}$
- We can thus use the methodology that has been developed for LMMs in this context.

- In matrix notation, the model can be rewrite as

$$\boldsymbol{y}_i = \boldsymbol{X}_i\boldsymbol{\beta} + \mathbf{1}_i\alpha_i + \boldsymbol{\epsilon}_i.$$

- $\mathrm{E}(\boldsymbol{y}_i) = \boldsymbol{X}_i\boldsymbol{\beta}$ and $\mathrm{Var}(\boldsymbol{y}_i) = \boldsymbol{V}_i$, where $\boldsymbol{V}_i = \sigma_\alpha^2 \mathbf{1}_{n_i}\mathbf{1}_{n_i}^T + \sigma^2 \boldsymbol{I}_{n_i}$.
- We then represent the vector of trail data for all vehicles:

$$\boldsymbol{y} = \boldsymbol{X}\boldsymbol{\beta} + \boldsymbol{Z}\boldsymbol{\alpha} + \boldsymbol{\epsilon}$$

  where $\boldsymbol{Z} = (\mathbf{1}_1, \ldots, \mathbf{1}_m)^T$.
- $\mathrm{E}(\boldsymbol{y}) = \boldsymbol{X}\boldsymbol{\beta}$ and $\mathrm{Var}(\boldsymbol{y}) = \boldsymbol{V}$, where $\boldsymbol{V} = \sigma_\alpha^2 \boldsymbol{Z}\boldsymbol{Z}^T + \sigma^2 \boldsymbol{I}$
- We can thus use the methodology that has been developed for LMMs in this context.

Outline

Likelihood inference and parameter estimation

- The estimation of the unknown coefficients $\boldsymbol{\beta}$ and $\boldsymbol{\alpha}$ clearly depends on the variance-covariance components σ_α^2 and σ^2.
- It is convenient to assume that both of $\boldsymbol{\alpha}$ and $\boldsymbol{\epsilon}$ are distributed normally.
- Then $\boldsymbol{y}$ has the normal distribution with mean vector $\boldsymbol{X\beta}$ and variance matrix $\boldsymbol{V}$.
- When σ_α^2 and σ^2 are known, then the estimator of $\boldsymbol{\beta}$ is the least squares estimator

$$\widehat{\boldsymbol{\beta}} = \left(\boldsymbol{X}^T\boldsymbol{V}^{-1}\boldsymbol{X}\right)^{-1}\boldsymbol{X}^T\boldsymbol{V}^{-1}\boldsymbol{y}, \tag{6}$$

and the estimator of $\hat{\boldsymbol{\alpha}}$ is the posterior mean

$$\widehat{\boldsymbol{\alpha}} = \sigma_\alpha^2\boldsymbol{Z}^T\boldsymbol{V}^{-1}(\boldsymbol{y} - \boldsymbol{X}\widehat{\boldsymbol{\beta}}), \tag{7}$$

where $\boldsymbol{V} = \sigma_\alpha^2\boldsymbol{Z}\boldsymbol{Z}^T + \sigma^2\boldsymbol{I}_n$.

Likelihood inference and parameter estimation

- The estimation of the unknown coefficients $\boldsymbol{\beta}$ and $\boldsymbol{\alpha}$ clearly depends on the variance-covariance components σ_α^2 and σ^2.
- It is convenient to assume that both of $\boldsymbol{\alpha}$ and $\boldsymbol{\epsilon}$ are distributed normally.
- Then $\boldsymbol{y}$ has the normal distribution with mean vector $\boldsymbol{X\beta}$ and variance matrix $\boldsymbol{V}$.
- When σ_α^2 and σ^2 are known, then the estimator of $\boldsymbol{\beta}$ is the least squares estimator

$$\widehat{\boldsymbol{\beta}} = \left(\boldsymbol{X}^T\boldsymbol{V}^{-1}\boldsymbol{X}\right)^{-1}\boldsymbol{X}^T\boldsymbol{V}^{-1}\boldsymbol{y}, \tag{6}$$

and the estimator of $\hat{\boldsymbol{\alpha}}$ is the posterior mean

$$\widehat{\boldsymbol{\alpha}} = \sigma_\alpha^2\boldsymbol{Z}^T\boldsymbol{V}^{-1}(\boldsymbol{y} - \boldsymbol{X}\widehat{\boldsymbol{\beta}}), \tag{7}$$

where $\boldsymbol{V} = \sigma_\alpha^2\boldsymbol{Z}\boldsymbol{Z}^T + \sigma^2\boldsymbol{I}_n$.

Likelihood inference and parameter estimation

- The estimation of the unknown coefficients $\boldsymbol{\beta}$ and $\boldsymbol{\alpha}$ clearly depends on the variance-covariance components σ_α^2 and σ^2.
- It is convenient to assume that both of $\boldsymbol{\alpha}$ and $\boldsymbol{\epsilon}$ are distributed normally.
- Then $\boldsymbol{y}$ has the normal distribution with mean vector $\boldsymbol{X\beta}$ and variance matrix $\boldsymbol{V}$.
- When σ_α^2 and σ^2 are known, then the estimator of β is the least squares estimator

$$\widehat{\boldsymbol{\beta}} = \left(\boldsymbol{X}^T\boldsymbol{V}^{-1}\boldsymbol{X}\right)^{-1}\boldsymbol{X}^T\boldsymbol{V}^{-1}\boldsymbol{y}, \tag{6}$$

and the estimator of $\hat{\alpha}$ is the posterior mean

$$\widehat{\boldsymbol{\alpha}} = \sigma_\alpha^2\boldsymbol{Z}^T\boldsymbol{V}^{-1}(\boldsymbol{y} - \boldsymbol{X}\widehat{\boldsymbol{\beta}}), \tag{7}$$

where $\boldsymbol{V} = \sigma_\alpha^2\boldsymbol{Z}\boldsymbol{Z}^T + \sigma^2\boldsymbol{I}_n$.

Likelihood inference and parameter estimation

- The estimation of the unknown coefficients $\boldsymbol{\beta}$ and $\boldsymbol{\alpha}$ clearly depends on the variance-covariance components σ_α^2 and σ^2.
- It is convenient to assume that both of $\boldsymbol{\alpha}$ and $\boldsymbol{\epsilon}$ are distributed normally.
- Then $\boldsymbol{y}$ has the normal distribution with mean vector $\boldsymbol{X\beta}$ and variance matrix $\boldsymbol{V}$.
- When σ_α^2 and σ^2 are known, then the estimator of $\boldsymbol{\beta}$ is the least squares estimator

$$\widehat{\boldsymbol{\beta}} = \left(\boldsymbol{X}^T\boldsymbol{V}^{-1}\boldsymbol{X}\right)^{-1}\boldsymbol{X}^T\boldsymbol{V}^{-1}\boldsymbol{y}, \tag{6}$$

and the estimator of $\hat{\boldsymbol{\alpha}}$ is the posterior mean

$$\widehat{\boldsymbol{\alpha}} = \sigma_\alpha^2\boldsymbol{Z}^T\boldsymbol{V}^{-1}(\boldsymbol{y} - \boldsymbol{X}\widehat{\boldsymbol{\beta}}), \tag{7}$$

where $\boldsymbol{V} = \sigma_\alpha^2\boldsymbol{Z}\boldsymbol{Z}^T + \sigma^2\boldsymbol{I}_n$.

- When σ_α^2 and σ^2 are unknown, we need to estimate σ_α^2 and σ^2 and replace them by their estimators $\hat{\sigma}_\alpha^2$ and $\hat{\sigma}^2$, and set $\widehat{\boldsymbol{V}} = \hat{\sigma}_\alpha^2 \boldsymbol{Z}\boldsymbol{Z}^T + \hat{\sigma}^2 \boldsymbol{I}$, then replace $\boldsymbol{V}$ by $\widehat{\boldsymbol{V}}$ in the above equations.
- The variance components σ_α^2 and σ^2 are estimated either using ML or REML.
- The marginal log-likelihood for computing ML estimates is given by

$$l(\boldsymbol{\beta}, \sigma_\alpha^2, \sigma^2) = -\frac{1}{2}\log|\boldsymbol{V}| - \frac{1}{2}(\boldsymbol{y} - \boldsymbol{X}\boldsymbol{\beta})^T \boldsymbol{V}^{-1}(\boldsymbol{y} - \boldsymbol{X}\boldsymbol{\beta}). \tag{8}$$

and similarly for REML is given by

$$l_R(\boldsymbol{\beta}, \sigma_\alpha^2, \sigma^2) = l(\boldsymbol{\beta}, \sigma_\alpha^2, \sigma^2) - \frac{1}{2}\log\left|\boldsymbol{X}^T \boldsymbol{V}^{-1} \boldsymbol{X}\right|. \tag{9}$$

- When σ_α^2 and σ^2 are unknown, we need to estimate σ_α^2 and σ^2 and replace them by their estimators $\hat{\sigma}_\alpha^2$ and $\hat{\sigma}^2$, and set $\widehat{\boldsymbol{V}} = \hat{\sigma}_\alpha^2 \boldsymbol{Z}\boldsymbol{Z}^T + \hat{\sigma}^2 \boldsymbol{I}$, then replace $\boldsymbol{V}$ by $\widehat{\boldsymbol{V}}$ in the above equations.
- The variance components σ_α^2 and σ^2 are estimated either using ML or REML.
- The marginal log-likelihood for computing ML estimates is given by

$$l(\boldsymbol{\beta}, \sigma_\alpha^2, \sigma^2) = -\frac{1}{2}\log|\boldsymbol{V}| - \frac{1}{2}(\boldsymbol{y} - \boldsymbol{X}\boldsymbol{\beta})^T \boldsymbol{V}^{-1}(\boldsymbol{y} - \boldsymbol{X}\boldsymbol{\beta}). \tag{8}$$

and similarly for REML is given by

$$l_R(\boldsymbol{\beta}, \sigma_\alpha^2, \sigma^2) = l(\boldsymbol{\beta}, \sigma_\alpha^2, \sigma^2) - \frac{1}{2}\log\left|\boldsymbol{X}^T \boldsymbol{V}^{-1} \boldsymbol{X}\right|. \tag{9}$$

- When σ_α^2 and σ^2 are unknown, we need to estimate σ_α^2 and σ^2 and replace them by their estimators $\hat{\sigma}_\alpha^2$ and $\hat{\sigma}^2$, and set $\widehat{\boldsymbol{V}} = \hat{\sigma}_\alpha^2 \boldsymbol{Z}\boldsymbol{Z}^T + \hat{\sigma}^2 \boldsymbol{I}$, then replace $\boldsymbol{V}$ by $\widehat{\boldsymbol{V}}$ in the above equations.
- The variance components σ_α^2 and σ^2 are estimated either using ML or REML.
- The marginal log-likelihood for computing ML estimates is given by

$$l(\boldsymbol{\beta}, \sigma_\alpha^2, \sigma^2) = -\frac{1}{2}\log|\boldsymbol{V}| - \frac{1}{2}(\boldsymbol{y} - \boldsymbol{X}\boldsymbol{\beta})^T \boldsymbol{V}^{-1}(\boldsymbol{y} - \boldsymbol{X}\boldsymbol{\beta}). \tag{8}$$

and similarly for REML is given by

$$l_R(\boldsymbol{\beta}, \sigma_\alpha^2, \sigma^2) = l(\boldsymbol{\beta}, \sigma_\alpha^2, \sigma^2) - \frac{1}{2}\log\left|\boldsymbol{X}^T \boldsymbol{V}^{-1} \boldsymbol{X}\right|. \tag{9}$$

- Since α_α^2 and σ^2 are rarely known, we need to estimate $\boldsymbol{\beta}, \sigma_\alpha^2$, and σ^2 simultaneously. This can be done by EM or Newton-Raphson algorithms for (8) and (9).
- Not numerically stable to estimate $\boldsymbol{\beta}$, σ_α^2, and σ^2 simultaneously.
- Another way is treating the unknown $\boldsymbol{\beta}$ as nuisance parameters to profile out the likelihood.
- Let $\boldsymbol{\theta} = (\sigma_\alpha^2, \sigma^2)^T$ and denote $\boldsymbol{V}(\boldsymbol{\theta})$ the variance $\boldsymbol{V}$ as a function of $\boldsymbol{\theta}$.
- The log-likelihood for $(\boldsymbol{\beta}, \boldsymbol{\theta})^T$ in (8) can be rewritten as:

$$l(\boldsymbol{\beta}, \boldsymbol{\theta}) = -\frac{1}{2}\log|\boldsymbol{V}(\boldsymbol{\theta})| - \frac{1}{2}(\boldsymbol{y} - \boldsymbol{X}\boldsymbol{\beta})^T(\boldsymbol{V}(\boldsymbol{\theta}))^{-1}(\boldsymbol{y} - \boldsymbol{X}\boldsymbol{\beta}). \quad (10)$$

- If we maximize (10) for fixed $\boldsymbol{\theta}$ with respect to $\boldsymbol{\beta}$, we get

$$\widetilde{\boldsymbol{\beta}}(\boldsymbol{\theta}) := \left(\boldsymbol{X}^T(\boldsymbol{V}(\boldsymbol{\theta}))^{-1}\boldsymbol{X}\right)^{-1}\boldsymbol{X}^T(\boldsymbol{V}(\boldsymbol{\theta}))^{-1}\boldsymbol{y},$$

which has exactly the same formula and analogous solution as we stated in (6).

- Since α_α^2 and σ^2 are rarely known, we need to estimate $\boldsymbol{\beta}, \sigma_\alpha^2$, and σ^2 simultaneously. This can be done by EM or Newton-Raphson algorithms for (8) and (9).
- Not numerically stable to estimate $\boldsymbol{\beta}$, σ_α^2, and σ^2 simultaneously.
- Another way is treating the unknown $\boldsymbol{\beta}$ as nuisance parameters to profile out the likelihood.
- Let $\boldsymbol{\theta} = (\sigma_\alpha^2, \sigma^2)^T$ and denote $\boldsymbol{V}(\boldsymbol{\theta})$ the variance $\boldsymbol{V}$ as a function of $\boldsymbol{\theta}$.
- The log-likelihood for $(\boldsymbol{\beta}, \boldsymbol{\theta})^T$ in (8) can be rewritten as:

$$l(\boldsymbol{\beta}, \boldsymbol{\theta}) = -\frac{1}{2}\log|\boldsymbol{V}(\boldsymbol{\theta})| - \frac{1}{2}(\boldsymbol{y} - \boldsymbol{X}\boldsymbol{\beta})^T(\boldsymbol{V}(\boldsymbol{\theta}))^{-1}(\boldsymbol{y} - \boldsymbol{X}\boldsymbol{\beta}). \quad (10)$$

- If we maximize (10) for fixed $\boldsymbol{\theta}$ with respect to $\boldsymbol{\beta}$, we get

$$\widetilde{\boldsymbol{\beta}}(\boldsymbol{\theta}) := \left(\boldsymbol{X}^T(\boldsymbol{V}(\boldsymbol{\theta}))^{-1}\boldsymbol{X}\right)^{-1}\boldsymbol{X}^T(\boldsymbol{V}(\boldsymbol{\theta}))^{-1}\boldsymbol{y},$$

which has exactly the same formula and analogous solution as we stated in (6).

- Since α_α^2 and σ^2 are rarely known, we need to estimate $\boldsymbol{\beta}, \sigma_\alpha^2$, and σ^2 simultaneously. This can be done by EM or Newton-Raphson algorithms for (8) and (9).
- Not numerically stable to estimate $\boldsymbol{\beta}$, σ_α^2, and σ^2 simultaneously.
- Another way is treating the unknown $\boldsymbol{\beta}$ as nuisance parameters to profile out the likelihood.
- Let $\boldsymbol{\theta} = (\sigma_\alpha^2, \sigma^2)^T$ and denote $\boldsymbol{V}(\boldsymbol{\theta})$ the variance $\boldsymbol{V}$ as a function of $\boldsymbol{\theta}$.
- The log-likelihood for $(\boldsymbol{\beta}, \boldsymbol{\theta})^T$ in (8) can be rewritten as:

$$l(\boldsymbol{\beta}, \boldsymbol{\theta}) = -\frac{1}{2}\log|\boldsymbol{V}(\boldsymbol{\theta})| - \frac{1}{2}(\boldsymbol{y} - \boldsymbol{X}\boldsymbol{\beta})^T(\boldsymbol{V}(\boldsymbol{\theta}))^{-1}(\boldsymbol{y} - \boldsymbol{X}\boldsymbol{\beta}). \quad (10)$$

- If we maximize (10) for fixed $\boldsymbol{\theta}$ with respect to $\boldsymbol{\beta}$, we get

$$\widetilde{\boldsymbol{\beta}}(\boldsymbol{\theta}) := \left(\boldsymbol{X}^T(\boldsymbol{V}(\boldsymbol{\theta}))^{-1}\boldsymbol{X}\right)^{-1}\boldsymbol{X}^T(\boldsymbol{V}(\boldsymbol{\theta}))^{-1}\boldsymbol{y},$$

which has exactly the same formula and analogous solution as we stated in (6).

- Since α_α^2 and σ^2 are rarely known, we need to estimate $\boldsymbol{\beta}, \sigma_\alpha^2$, and σ^2 simultaneously. This can be done by EM or Newton-Raphson algorithms for (8) and (9).
- Not numerically stable to estimate $\boldsymbol{\beta}$, σ_α^2, and σ^2 simultaneously.
- Another way is treating the unknown $\boldsymbol{\beta}$ as nuisance parameters to profile out the likelihood.
- Let $\boldsymbol{\theta} = (\sigma_\alpha^2, \sigma^2)^T$ and denote $\boldsymbol{V}(\boldsymbol{\theta})$ the variance $\boldsymbol{V}$ as a function of $\boldsymbol{\theta}$.
- The log-likelihood for $(\boldsymbol{\beta}, \boldsymbol{\theta})^T$ in (8) can be rewritten as:

$$l(\boldsymbol{\beta}, \boldsymbol{\theta}) = -\frac{1}{2}\log|\boldsymbol{V}(\boldsymbol{\theta})| - \frac{1}{2}(\boldsymbol{y} - \boldsymbol{X}\boldsymbol{\beta})^T(\boldsymbol{V}(\boldsymbol{\theta}))^{-1}(\boldsymbol{y} - \boldsymbol{X}\boldsymbol{\beta}). \quad (10)$$

- If we maximize (10) for fixed $\boldsymbol{\theta}$ with respect to $\boldsymbol{\beta}$, we get

$$\widetilde{\boldsymbol{\beta}}(\boldsymbol{\theta}) := \left(\boldsymbol{X}^T(\boldsymbol{V}(\boldsymbol{\theta}))^{-1}\boldsymbol{X}\right)^{-1}\boldsymbol{X}^T(\boldsymbol{V}(\boldsymbol{\theta}))^{-1}\boldsymbol{y},$$

which has exactly the same formula and analogous solution as we stated in (6).

- Since α_α^2 and σ^2 are rarely known, we need to estimate $\boldsymbol{\beta}, \sigma_\alpha^2$, and σ^2 simultaneously. This can be done by EM or Newton-Raphson algorithms for (8) and (9).
- Not numerically stable to estimate $\boldsymbol{\beta}$, σ_α^2, and σ^2 simultaneously.
- Another way is treating the unknown $\boldsymbol{\beta}$ as nuisance parameters to profile out the likelihood.
- Let $\boldsymbol{\theta} = (\sigma_\alpha^2, \sigma^2)^T$ and denote $\boldsymbol{V}(\boldsymbol{\theta})$ the variance $\boldsymbol{V}$ as a function of $\boldsymbol{\theta}$.
- The log-likelihood for $(\boldsymbol{\beta}, \boldsymbol{\theta})^T$ in (8) can be rewritten as:

$$l(\boldsymbol{\beta}, \boldsymbol{\theta}) = -\frac{1}{2}\log|\boldsymbol{V}(\boldsymbol{\theta})| - \frac{1}{2}(\boldsymbol{y} - \boldsymbol{X}\boldsymbol{\beta})^T(\boldsymbol{V}(\boldsymbol{\theta}))^{-1}(\boldsymbol{y} - \boldsymbol{X}\boldsymbol{\beta}). \qquad (10)$$

- If we maximize (10) for fixed $\boldsymbol{\theta}$ with respect to $\boldsymbol{\beta}$, we get

$$\widetilde{\boldsymbol{\beta}}(\boldsymbol{\theta}) := \left(\boldsymbol{X}^T(\boldsymbol{V}(\boldsymbol{\theta}))^{-1}\boldsymbol{X}\right)^{-1}\boldsymbol{X}^T(\boldsymbol{V}(\boldsymbol{\theta}))^{-1}\boldsymbol{y},$$

which has exactly the same formula and analogous solution as we stated in (6).

- Since α_α^2 and σ^2 are rarely known, we need to estimate $\boldsymbol{\beta}, \sigma_\alpha^2$, and σ^2 simultaneously. This can be done by EM or Newton-Raphson algorithms for (8) and (9).
- Not numerically stable to estimate $\boldsymbol{\beta}$, σ_α^2, and σ^2 simultaneously.
- Another way is treating the unknown $\boldsymbol{\beta}$ as nuisance parameters to profile out the likelihood.
- Let $\boldsymbol{\theta} = (\sigma_\alpha^2, \sigma^2)^T$ and denote $\boldsymbol{V}(\boldsymbol{\theta})$ the variance $\boldsymbol{V}$ as a function of $\boldsymbol{\theta}$.
- The log-likelihood for $(\boldsymbol{\beta}, \boldsymbol{\theta})^T$ in (8) can be rewritten as:

$$l(\boldsymbol{\beta}, \boldsymbol{\theta}) = -\frac{1}{2}\log|\boldsymbol{V}(\boldsymbol{\theta})| - \frac{1}{2}(\boldsymbol{y} - \boldsymbol{X}\boldsymbol{\beta})^T(\boldsymbol{V}(\boldsymbol{\theta}))^{-1}(\boldsymbol{y} - \boldsymbol{X}\boldsymbol{\beta}). \qquad (10)$$

- If we maximize (10) for fixed $\boldsymbol{\theta}$ with respect to $\boldsymbol{\beta}$, we get

$$\widetilde{\boldsymbol{\beta}}(\boldsymbol{\theta}) := \left(\boldsymbol{X}^T(\boldsymbol{V}(\boldsymbol{\theta}))^{-1}\boldsymbol{X}\right)^{-1}\boldsymbol{X}^T(\boldsymbol{V}(\boldsymbol{\theta}))^{-1}\boldsymbol{y},$$

which has exactly the same formula and analogous solution as we stated in (6).

- Replacing the $\boldsymbol{\beta}$ with $\widetilde{\boldsymbol{\beta}}(\boldsymbol{\theta})$ in (10), we derive the profile log-likelihood

$$l_P(\boldsymbol{\theta}) \coloneqq -\frac{1}{2}\log|\boldsymbol{V}(\boldsymbol{\theta})| - \frac{1}{2}(\boldsymbol{y}-\boldsymbol{X}\widetilde{\boldsymbol{\beta}}(\boldsymbol{\theta}))^T(\boldsymbol{V}(\boldsymbol{\theta}))^{-1}(\boldsymbol{y}-\boldsymbol{X}\widetilde{\boldsymbol{\beta}}(\boldsymbol{\theta})). \quad (11)$$

- The profile log-likelihood for REML estimates becomes

$$l_R(\boldsymbol{\theta}) = l_P(\boldsymbol{\theta}) - \frac{1}{2}\log|\boldsymbol{X}^T(\boldsymbol{V}(\boldsymbol{\theta}))^{-1}\boldsymbol{X}|. \quad (12)$$

- The variance parameters $\boldsymbol{\theta}$ are estimated by $\widehat{\boldsymbol{\theta}}$ which maximizes l_R in (12).
- The estimates of $\boldsymbol{\beta}$ are

$$\widehat{\boldsymbol{\beta}} = \left(\boldsymbol{X}^T\widehat{\boldsymbol{V}}^{-1}\boldsymbol{X}\right)\boldsymbol{X}^T\widehat{\boldsymbol{V}}^{-1}y,$$

and similarly the predictions of $\boldsymbol{\alpha}$ are

$$\widehat{\boldsymbol{\alpha}} = \hat{\sigma}_\alpha^2\boldsymbol{Z}^T\widehat{\boldsymbol{V}}^{-1}(y-\boldsymbol{X}\widehat{\boldsymbol{\beta}}),$$

where $\widehat{\boldsymbol{V}} = \boldsymbol{V}(\widehat{\boldsymbol{\theta}})$.

- Replacing the $\boldsymbol{\beta}$ with $\widetilde{\boldsymbol{\beta}}(\boldsymbol{\theta})$ in (10), we derive the profile log-likelihood

$$l_P(\boldsymbol{\theta}) \coloneqq -\frac{1}{2}\log|\boldsymbol{V}(\boldsymbol{\theta})| - \frac{1}{2}(\boldsymbol{y} - \boldsymbol{X}\widetilde{\boldsymbol{\beta}}(\boldsymbol{\theta}))^T(\boldsymbol{V}(\boldsymbol{\theta}))^{-1}(\boldsymbol{y} - \boldsymbol{X}\widetilde{\boldsymbol{\beta}}(\boldsymbol{\theta})). \quad (11)$$

- The profile log-likelihood for REML estimates becomes

$$l_R(\boldsymbol{\theta}) = l_P(\boldsymbol{\theta}) - \frac{1}{2}\log|\boldsymbol{X}^T(\boldsymbol{V}(\boldsymbol{\theta}))^{-1}\boldsymbol{X}|. \quad (12)$$

- The variance parameters θ are estimated by $\widehat{\theta}$ which maximizes l_R in (12).
- The estimates of β are

$$\widehat{\beta} = \left(\boldsymbol{X}^T\widehat{\boldsymbol{V}}^{-1}\boldsymbol{X}\right)\boldsymbol{X}^T\widehat{\boldsymbol{V}}^{-1}y,$$

and similarly the predictions of α are

$$\widehat{\boldsymbol{\alpha}} = \hat{\sigma}_\alpha^2\boldsymbol{Z}^T\widehat{\boldsymbol{V}}^{-1}(y - \boldsymbol{X}\widehat{\boldsymbol{\beta}}),$$

where $\widehat{\boldsymbol{V}} = \boldsymbol{V}(\widehat{\theta})$.

- Replacing the $\boldsymbol{\beta}$ with $\widetilde{\boldsymbol{\beta}}(\boldsymbol{\theta})$ in (10), we derive the profile log-likelihood

$$l_P(\boldsymbol{\theta}) := -\frac{1}{2}\log|\boldsymbol{V}(\boldsymbol{\theta})| - \frac{1}{2}(\boldsymbol{y} - \boldsymbol{X}\widetilde{\boldsymbol{\beta}}(\boldsymbol{\theta}))^T(\boldsymbol{V}(\boldsymbol{\theta}))^{-1}(\boldsymbol{y} - \boldsymbol{X}\widetilde{\boldsymbol{\beta}}(\boldsymbol{\theta})). \quad (11)$$

- The profile log-likelihood for REML estimates becomes

$$l_R(\boldsymbol{\theta}) = l_P(\boldsymbol{\theta}) - \frac{1}{2}\log|\boldsymbol{X}^T(\boldsymbol{V}(\boldsymbol{\theta}))^{-1}\boldsymbol{X}|. \quad (12)$$

- The variance parameters $\boldsymbol{\theta}$ are estimated by $\widehat{\boldsymbol{\theta}}$ which maximizes l_R in (12).
- The estimates of β are

$$\widehat{\beta} = \left(\boldsymbol{X}^T\widehat{\boldsymbol{V}}^{-1}\boldsymbol{X}\right)\boldsymbol{X}^T\widehat{\boldsymbol{V}}^{-1}y,$$

and similarly the predictions of $\boldsymbol{\alpha}$ are

$$\widehat{\boldsymbol{\alpha}} = \hat{\sigma}_\alpha^2\boldsymbol{Z}^T\widehat{\boldsymbol{V}}^{-1}(y - \boldsymbol{X}\widehat{\beta}),$$

where $\widehat{\boldsymbol{V}} = \boldsymbol{V}(\widehat{\theta})$.

- Replacing the $\boldsymbol{\beta}$ with $\widetilde{\boldsymbol{\beta}}(\boldsymbol{\theta})$ in (10), we derive the profile log-likelihood

$$l_P(\boldsymbol{\theta}) := -\frac{1}{2}\log|\boldsymbol{V}(\boldsymbol{\theta})| - \frac{1}{2}(\boldsymbol{y} - \boldsymbol{X}\widetilde{\boldsymbol{\beta}}(\boldsymbol{\theta}))^T(\boldsymbol{V}(\boldsymbol{\theta}))^{-1}(\boldsymbol{y} - \boldsymbol{X}\widetilde{\boldsymbol{\beta}}(\boldsymbol{\theta})). \quad (11)$$

- The profile log-likelihood for REML estimates becomes

$$l_R(\boldsymbol{\theta}) = l_P(\boldsymbol{\theta}) - \frac{1}{2}\log|\boldsymbol{X}^T(\boldsymbol{V}(\boldsymbol{\theta}))^{-1}\boldsymbol{X}|. \quad (12)$$

- The variance parameters $\boldsymbol{\theta}$ are estimated by $\widehat{\boldsymbol{\theta}}$ which maximizes l_R in (12).
- The estimates of $\boldsymbol{\beta}$ are

$$\widehat{\boldsymbol{\beta}} = \left(\boldsymbol{X}^T\widehat{\boldsymbol{V}}^{-1}\boldsymbol{X}\right)\boldsymbol{X}^T\widehat{\boldsymbol{V}}^{-1}\boldsymbol{y},$$

and similarly the predictions of $\boldsymbol{\alpha}$ are

$$\widehat{\boldsymbol{\alpha}} = \hat{\sigma}_\alpha^2\boldsymbol{Z}^T\widehat{\boldsymbol{V}}^{-1}(\boldsymbol{y} - \boldsymbol{X}\widehat{\boldsymbol{\beta}}),$$

where $\widehat{\boldsymbol{V}} = \boldsymbol{V}(\widehat{\boldsymbol{\theta}})$.

- There is no simple one-step solution. REML estimation of $\boldsymbol{\theta}$ requires an iterative procedure.
- we adopt the Newton-Raphson algorithm to estimate θ in (12) and apply the orthogonality convergence criterion to determine convergence.
- To make the iterations converge quickly, we use the results of $\widehat{\theta}$ from previous time t_{k-1} as a reasonable initial value for iterations at time t_k.

- There is no simple one-step solution. REML estimation of $\boldsymbol{\theta}$ requires an iterative procedure.
- we adopt the Newton-Raphson algorithm to estimate $\boldsymbol{\theta}$ in (12) and apply the orthogonality convergence criterion to determine convergence.
- To make the iterations converge quickly, we use the results of $\widehat{\theta}$ from previous time t_{k-1} as a reasonable initial value for iterations at time t_k.

- There is no simple one-step solution. REML estimation of $\boldsymbol{\theta}$ requires an iterative procedure.
- we adopt the Newton-Raphson algorithm to estimate $\boldsymbol{\theta}$ in (12) and apply the orthogonality convergence criterion to determine convergence.
- To make the iterations converge quickly, we use the results of $\widehat{\boldsymbol{\theta}}$ from previous time t_{k-1} as a reasonable initial value for iterations at time t_k.

Outline

Experimental evaluation

- We use NGSIM US-101 and I-80 datasets for our experiments.
- The detail description of the dataset is available here: https://ops.fhwa.dot.gov/trafficanalysistools/ngsim.htm
- The scope of the road shape is limited to a single road. Leading vehicles taking forks or exits are excluded from the estimation of the road model.
- Overall, 5 lanes and 5047 vehicles were analyzed for the US-101 dataset and 6 lanes and 5033 vehicles were analyzed for the I-80 dataset.
- The ground truth (lane centerline) was generated by excluding trajectories of lane-changing vehicles and fitting all in-lane trajectories with a smoothing spline function.
- The performance of the DRS will be measured by comparing it to the generated ground truth.

Experimental evaluation

- We use NGSIM US-101 and I-80 datasets for our experiments.
- The detail description of the dataset is available here: https://ops.fhwa.dot.gov/trafficanalysistools/ngsim.htm
- The scope of the road shape is limited to a single road. Leading vehicles taking forks or exits are excluded from the estimation of the road model.
- Overall, 5 lanes and 5047 vehicles were analyzed for the US-101 dataset and 6 lanes and 5033 vehicles were analyzed for the I-80 dataset.
- The ground truth (lane centerline) was generated by excluding trajectories of lane-changing vehicles and fitting all in-lane trajectories with a smoothing spline function.
- The performance of the DRS will be measured by comparing it to the generated ground truth.

Experimental evaluation

- We use NGSIM US-101 and I-80 datasets for our experiments.
- The detail description of the dataset is available here: https://ops.fhwa.dot.gov/trafficanalysistools/ngsim.htm
- The scope of the road shape is limited to a single road. Leading vehicles taking forks or exits are excluded from the estimation of the road model.
- Overall, 5 lanes and 5047 vehicles were analyzed for the US-101 dataset and 6 lanes and 5033 vehicles were analyzed for the I-80 dataset.
- The ground truth (lane centerline) was generated by excluding trajectories of lane-changing vehicles and fitting all in-lane trajectories with a smoothing spline function.
- The performance of the DRS will be measured by comparing it to the generated ground truth.

Experimental evaluation

- We use NGSIM US-101 and I-80 datasets for our experiments.
- The detail description of the dataset is available here: https://ops.fhwa.dot.gov/trafficanalysistools/ngsim.htm
- The scope of the road shape is limited to a single road. Leading vehicles taking forks or exits are excluded from the estimation of the road model.
- Overall, 5 lanes and 5047 vehicles were analyzed for the US-101 dataset and 6 lanes and 5033 vehicles were analyzed for the I-80 dataset.
- The ground truth (lane centerline) was generated by excluding trajectories of lane-changing vehicles and fitting all in-lane trajectories with a smoothing spline function.
- The performance of the DRS will be measured by comparing it to the generated ground truth.

Experimental evaluation

- We use NGSIM US-101 and I-80 datasets for our experiments.
- The detail description of the dataset is available here: https://ops.fhwa.dot.gov/trafficanalysistools/ngsim.htm
- The scope of the road shape is limited to a single road. Leading vehicles taking forks or exits are excluded from the estimation of the road model.
- Overall, 5 lanes and 5047 vehicles were analyzed for the US-101 dataset and 6 lanes and 5033 vehicles were analyzed for the I-80 dataset.
- The ground truth (lane centerline) was generated by excluding trajectories of lane-changing vehicles and fitting all in-lane trajectories with a smoothing spline function.
- The performance of the DRS will be measured by comparing it to the generated ground truth.

Experimental evaluation

- We use NGSIM US-101 and I-80 datasets for our experiments.
- The detail description of the dataset is available here: https://ops.fhwa.dot.gov/trafficanalysistools/ngsim.htm
- The scope of the road shape is limited to a single road. Leading vehicles taking forks or exits are excluded from the estimation of the road model.
- Overall, 5 lanes and 5047 vehicles were analyzed for the US-101 dataset and 6 lanes and 5033 vehicles were analyzed for the I-80 dataset.
- The ground truth (lane centerline) was generated by excluding trajectories of lane-changing vehicles and fitting all in-lane trajectories with a smoothing spline function.
- The performance of the DRS will be measured by comparing it to the generated ground truth.

Data preparation and process

- For each simulation run, we treat one vehicle as the host vehicle and other vehicles as guests.
- For the host vehicle at each time step k, the global position (x^g_{hk}, y^g_{hk}) is directly from the dataset and the orientation ψ^g_{hk} is estimated from two consecutive points (preprocessed and smoothed).
- The host vehicle is attached with a local coordinate frame l_k and its position is always at the origin in the local coordinate frame.
- For the i-th guest vehicle at time step k, we use the global position (x^g_{ik}, y^g_{ik}) from the dataset to convert it into the local coordinate $(x^{l_k}_{ik}, y^{l_k}_{ik})$ by using (1). This conversion happens for every time step k.

Data preparation and process

- For each simulation run, we treat one vehicle as the host vehicle and other vehicles as guests.
- For the host vehicle at each time step k, the global position (x^g_{hk}, y^g_{hk}) is directly from the dataset and the orientation ψ^g_{hk} is estimated from two consecutive points (preprocessed and smoothed).
- The host vehicle is attached with a local coordinate frame l_k and its position is always at the origin in the local coordinate frame.
- For the i-th guest vehicle at time step k, we use the global position (x^g_{ik}, y^g_{ik}) from the dataset to convert it into the local coordinate $(x^{l_k}_{ik}, y^{l_k}_{ik})$ by using (1). This conversion happens for every time step k.

Data preparation and process

- For each simulation run, we treat one vehicle as the host vehicle and other vehicles as guests.
- For the host vehicle at each time step k, the global position (x^g_{hk}, y^g_{hk}) is directly from the dataset and the orientation ψ^g_{hk} is estimated from two consecutive points (preprocessed and smoothed).
- The host vehicle is attached with a local coordinate frame l_k and its position is always at the origin in the local coordinate frame.
- For the i-th guest vehicle at time step k, we use the global position (x^g_{ik}, y^g_{ik}) from the dataset to convert it into the local coordinate $(x^{l_k}_{ik}, y^{l_k}_{ik})$ by using (1). This conversion happens for every time step k.

Data preparation and process

- For each simulation run, we treat one vehicle as the host vehicle and other vehicles as guests.
- For the host vehicle at each time step k, the global position (x^g_{hk}, y^g_{hk}) is directly from the dataset and the orientation ψ^g_{hk} is estimated from two consecutive points (preprocessed and smoothed).
- The host vehicle is attached with a local coordinate frame l_k and its position is always at the origin in the local coordinate frame.
- For the i-th guest vehicle at time step k, we use the global position (x^g_{ik}, y^g_{ik}) from the dataset to convert it into the local coordinate $(x^{l_k}_{ik}, y^{l_k}_{ik})$ by using (1). This conversion happens for every time step k.

(a) FoV and tracked vehicles

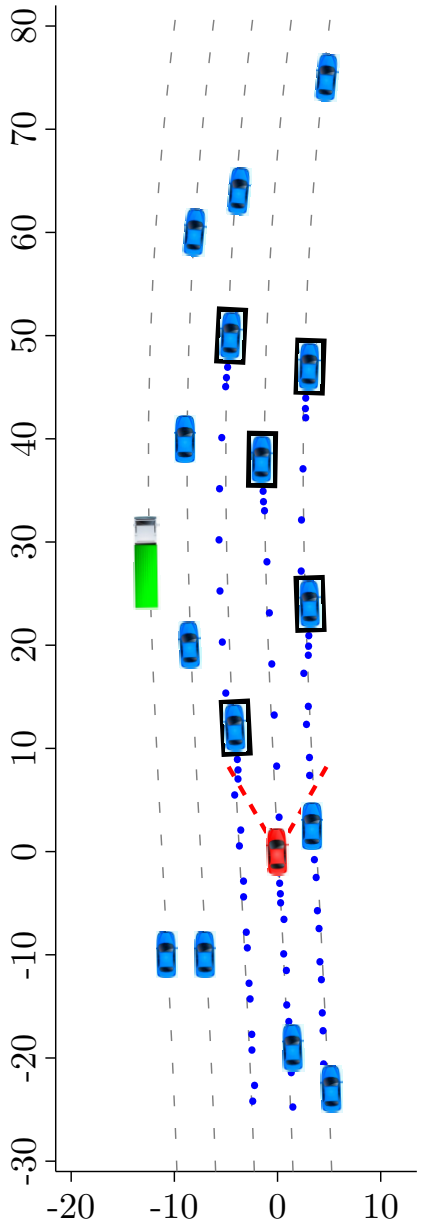

(b) Aligned DRS and GT

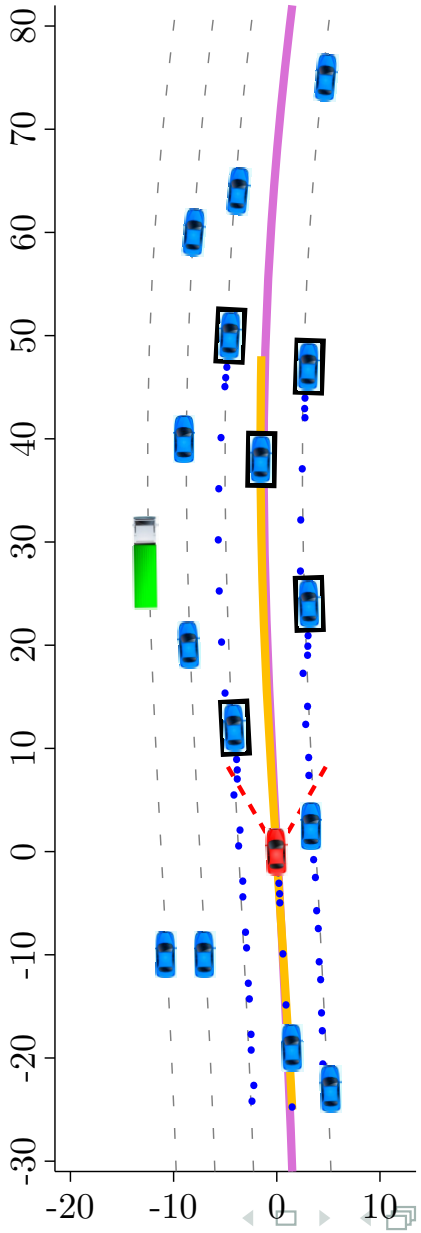

Performance measure

- We use the root mean square error (RMSE) to calculate the lateral difference between the estimated DRS and the ground truth.
- The RMSE is defined as

$$\text{RMSE} = \sqrt{\frac{1}{K}\sum_{k=1}^{K}(\hat{y}_k - y_k)^2},$$

  where $\hat{y}_k$ is the lateral value of estimated DRS and y_k is the lateral value of the ground truth.
- We report the value of RMSE downrange from 10 to 100 meters ahead of the road, sampled every 10 meters, for each simulation run.

Performance measure

- We use the root mean square error (RMSE) to calculate the lateral difference between the estimated DRS and the ground truth.
- The RMSE is defined as

$$\text{RMSE} = \sqrt{\frac{1}{K}\sum_{k=1}^{K}(\hat{y}_k - y_k)^2},$$

  where $\hat{y}_k$ is the lateral value of estimated DRS and y_k is the lateral value of the ground truth.
- We report the value of RMSE downrange from 10 to 100 meters ahead of the road, sampled every 10 meters, for each simulation run.

Performance measure

- We use the root mean square error (RMSE) to calculate the lateral difference between the estimated DRS and the ground truth.
- The RMSE is defined as

$$\text{RMSE} = \sqrt{\frac{1}{K}\sum_{k=1}^{K}(\hat{y}_k - y_k)^2},$$

  where $\hat{y}_k$ is the lateral value of estimated DRS and y_k is the lateral value of the ground truth.
- We report the value of RMSE downrange from 10 to 100 meters ahead of the road, sampled every 10 meters, for each simulation run.

(a) US-101 dataset

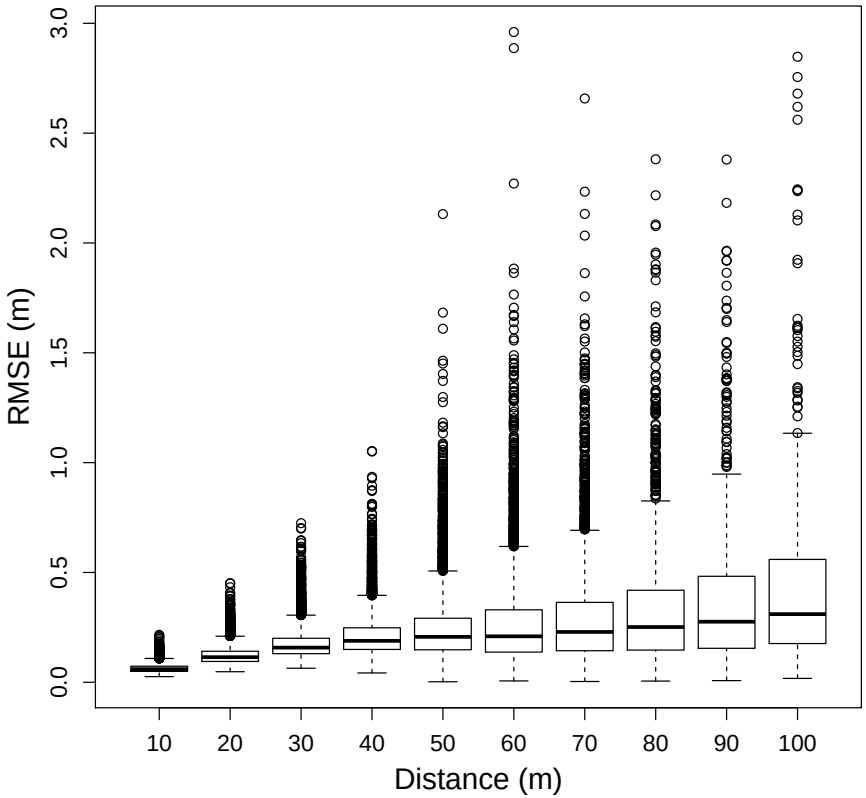

(b) I-80 dataset

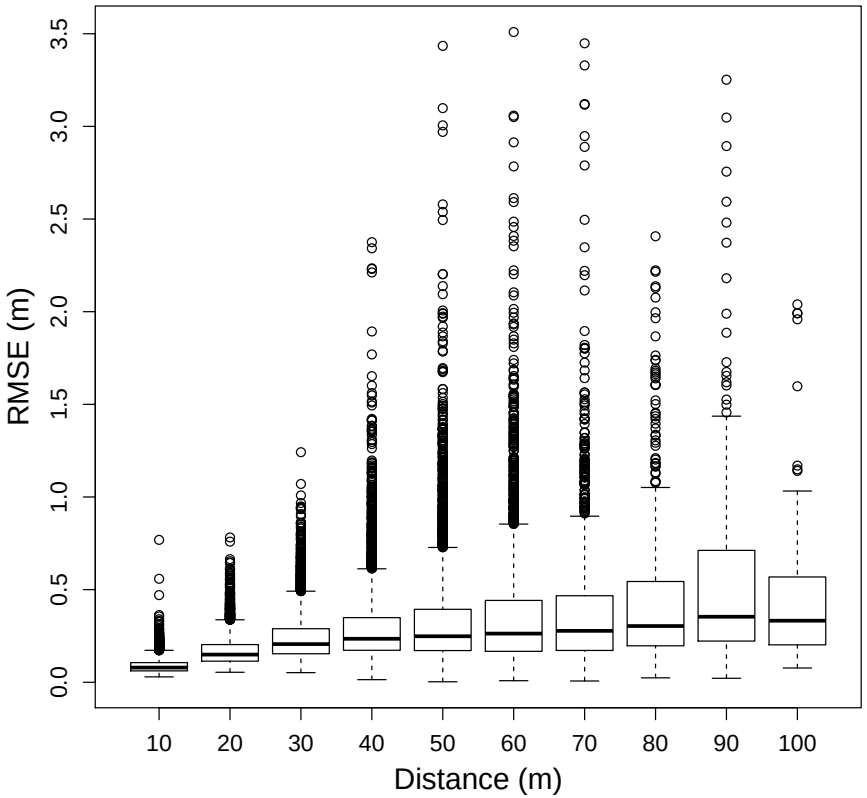

Figure: Boxplot of RMSE with different distances ahead of the road for (a) US-101 dataset with 5047 simulation runs and (b) I-80 dataset with 5033 simulation runs.

(a) A lane change trail

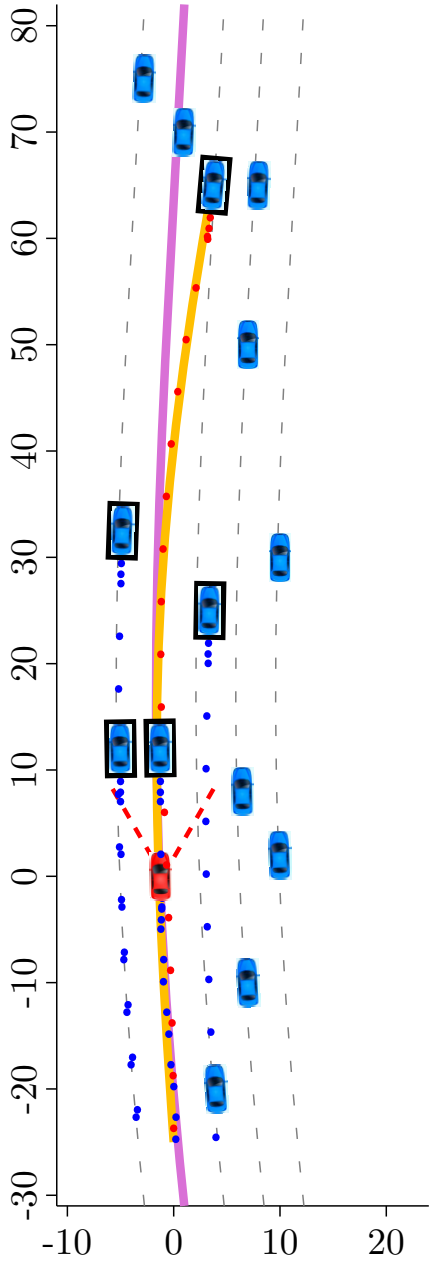

(b) A gap between trails

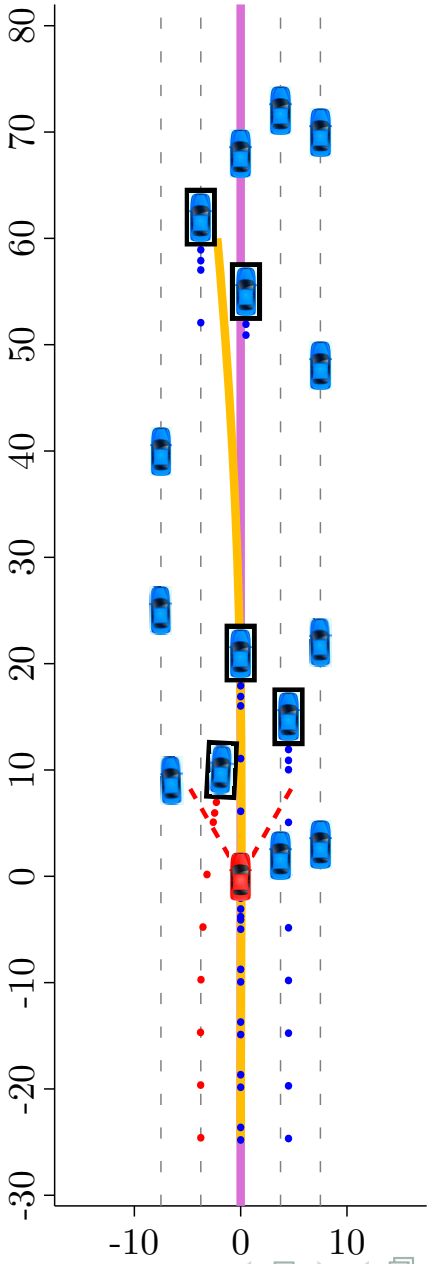

Effects of trail compression and lane-changing vehicles

- To explore the effects of the trail compression on the estimated DRS, as well as how lane-changing vehicles affect the behavior of the estimated DRS, we investigate the performance by comparing the following methods:
  - DRS: The trail samples were compressed and chopped.
  - DRS_u: The trail samples were processed with the trail chopping but without the trail compression. The subscript u means uncompressed.
  - DRS_0: Same as the DRS, but the trails from lane-changing vehicles were excluded from the LMM process.
  - DRS_{u0}: Same as the DRS_u, but the trails from lane-changing vehicles were excluded from the LMM process.
- For ease of comparison, we calculate the sample means with the associated standard errors of the RMSE values for the above four methods at different distances.

Effects of trail compression and lane-changing vehicles

- To explore the effects of the trail compression on the estimated DRS, as well as how lane-changing vehicles affect the behavior of the estimated DRS, we investigate the performance by comparing the following methods:
  - DRS: The trail samples were compressed and chopped.
  - DRS_u: The trail samples were processed with the trail chopping but without the trail compression. The subscript u means uncompressed.
  - DRS_0: Same as the DRS, but the trails from lane-changing vehicles were excluded from the LMM process.
  - DRS_{u0}: Same as the DRS_u, but the trails from lane-changing vehicles were excluded from the LMM process.
- For ease of comparison, we calculate the sample means with the associated standard errors of the RMSE values for the above four methods at different distances.

Effects of trail compression and lane-changing vehicles

- To explore the effects of the trail compression on the estimated DRS, as well as how lane-changing vehicles affect the behavior of the estimated DRS, we investigate the performance by comparing the following methods:
  - DRS: The trail samples were compressed and chopped.
  - DRS$_u$: The trail samples were processed with the trail chopping but without the trail compression. The subscript u means uncompressed.
  - DRS$_0$: Same as the DRS, but the trails from lane-changing vehicles were excluded from the LMM process.
  - DRS$_{u0}$: Same as the DRS$_u$, but the trails from lane-changing vehicles were excluded from the LMM process.
- For ease of comparison, we calculate the sample means with the associated standard errors of the RMSE values for the above four methods at different distances.

Effects of trail compression and lane-changing vehicles

- To explore the effects of the trail compression on the estimated DRS, as well as how lane-changing vehicles affect the behavior of the estimated DRS, we investigate the performance by comparing the following methods:
  - DRS: The trail samples were compressed and chopped.
  - DRS$_u$: The trail samples were processed with the trail chopping but without the trail compression. The subscript u means uncompressed.
  - DRS$_0$: Same as the DRS, but the trails from lane-changing vehicles were excluded from the LMM process.
  - DRS$_{u0}$: Same as the DRS$_u$, but the trails from lane-changing vehicles were excluded from the LMM process.
- For ease of comparison, we calculate the sample means with the associated standard errors of the RMSE values for the above four methods at different distances.

Effects of trail compression and lane-changing vehicles

- To explore the effects of the trail compression on the estimated DRS, as well as how lane-changing vehicles affect the behavior of the estimated DRS, we investigate the performance by comparing the following methods:
  - DRS: The trail samples were compressed and chopped.
  - DRS$_u$: The trail samples were processed with the trail chopping but without the trail compression. The subscript u means uncompressed.
  - DRS$_0$: Same as the DRS, but the trails from lane-changing vehicles were excluded from the LMM process.
  - DRS$_{u0}$: Same as the DRS$_u$, but the trails from lane-changing vehicles were excluded from the LMM process.
- For ease of comparison, we calculate the sample means with the associated standard errors of the RMSE values for the above four methods at different distances.

Effects of trail compression and lane-changing vehicles

- To explore the effects of the trail compression on the estimated DRS, as well as how lane-changing vehicles affect the behavior of the estimated DRS, we investigate the performance by comparing the following methods:
  - DRS: The trail samples were compressed and chopped.
  - DRS_u: The trail samples were processed with the trail chopping but without the trail compression. The subscript u means uncompressed.
  - DRS_0: Same as the DRS, but the trails from lane-changing vehicles were excluded from the LMM process.
  - DRS_{u0}: Same as the DRS_u, but the trails from lane-changing vehicles were excluded from the LMM process.
- For ease of comparison, we calculate the sample means with the associated standard errors of the RMSE values for the above four methods at different distances.

Table: The offset difference of the estimated DRS compared to ground truth at each distance in terms of averaged RMSE (standard error in parenthesis) with/without the trail compression and with/without lane-changing vehicles for both datasets.

US-101	Distance (m)									
	10	20	30	40	50	60	70	80	90	100
DRS	0.0640 (0.0212)	0.1239 (0.0441)	0.1763 (0.0724)	0.2162 (0.1056)	0.2489 (0.1662)	0.2754 (0.2307)	0.3070 (0.2677)	0.3503 (0.3194)	0.3851 (0.3526)	0.4718 (0.4865)
DRS_u	0.0653 (0.0224)	0.1283 (0.0488)	0.1868 (0.0805)	0.2316 (0.1157)	0.2670 (0.1828)	0.2942 (0.2537)	0.3258 (0.2873)	0.3727 (0.3430)	0.4123 (0.3766)	0.5032 (0.5163)
DRS_0	0.0590 (0.0173)	0.1121 (0.0309)	0.1532 (0.0432)	0.1806 (0.0654)	0.1983 (0.1049)	0.2139 (0.1414)	0.2357 (0.1719)	0.2706 (0.2192)	0.3036 (0.2721)	0.3485 (0.3460)
DRS_{u0}	0.0608 (0.0180)	0.1168 (0.0328)	0.1633 (0.0472)	0.1949 (0.0710)	0.2140 (0.1136)	0.2299 (0.1534)	0.2511 (0.1837)	0.2887 (0.2355)	0.3271 (0.2914)	0.3765 (0.3704)

Table: The offset difference of the estimated DRS compared to ground truth at each distance in terms of averaged RMSE (standard error in parenthesis) with/without the trail compression and with/without lane-changing vehicles for both datasets.

I-80	Distance (m)									
	10	20	30	40	50	60	70	80	90	100
DRS	0.0892 (0.0413)	0.1705 (0.0821)	0.2437 (0.1322)	0.2970 (0.2074)	0.3352 (0.2875)	0.3719 (0.3530)	0.4020 (0.4003)	0.4566 (0.4272)	0.5651 (0.5755)	0.4914 (0.4466)
DRS_u	0.0928 (0.0443)	0.1805 (0.0918)	0.2637 (0.1498)	0.3225 (0.2319)	0.3626 (0.3199)	0.3996 (0.3830)	0.4354 (0.4825)	0.4806 (0.4534)	0.5977 (0.6839)	0.5134 (0.4571)
DRS_0	0.0761 (0.0342)	0.1404 (0.0448)	0.1893 (0.1018)	0.2273 (0.1536)	0.2558 (0.2434)	0.2863 (0.3067)	0.3295 (0.3543)	0.4091 (0.3753)	0.4278 (0.4498)	0.4110 (0.3655)
DRS_{u0}	0.0795 (0.0783)	0.1486 (0.1281)	0.2042 (0.1720)	0.2464 (0.2336)	0.2755 (0.3190)	0.3079 (0.2444)	0.3518 (0.3127)	0.4284 (0.4062)	0.4694 (0.4364)	0.4572 (0.3789)

(a) US-101 dataset

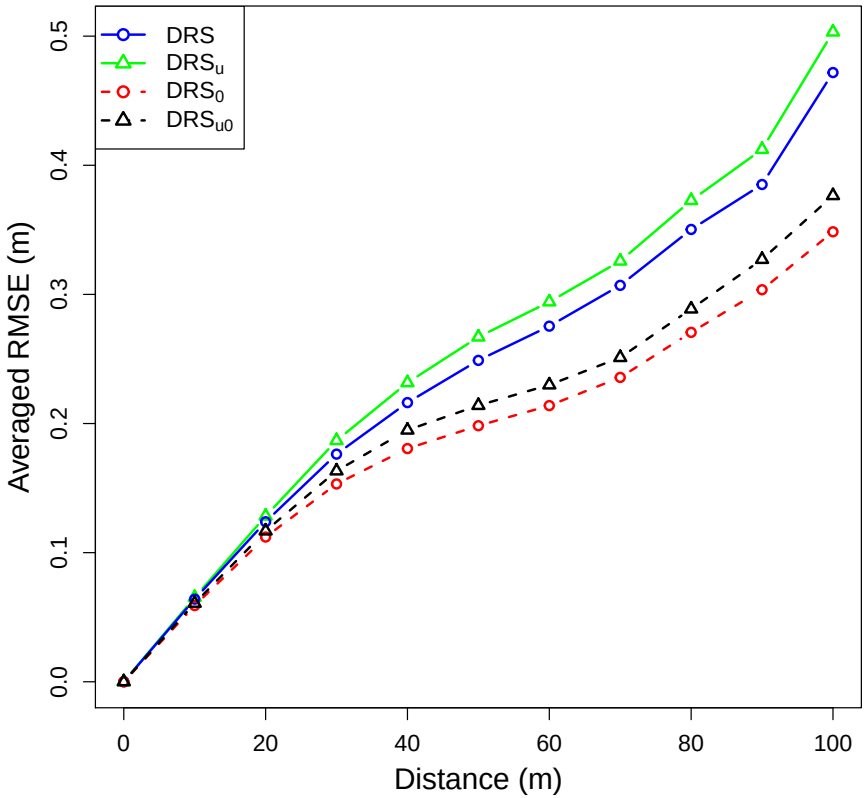

(b) I-80 dataset

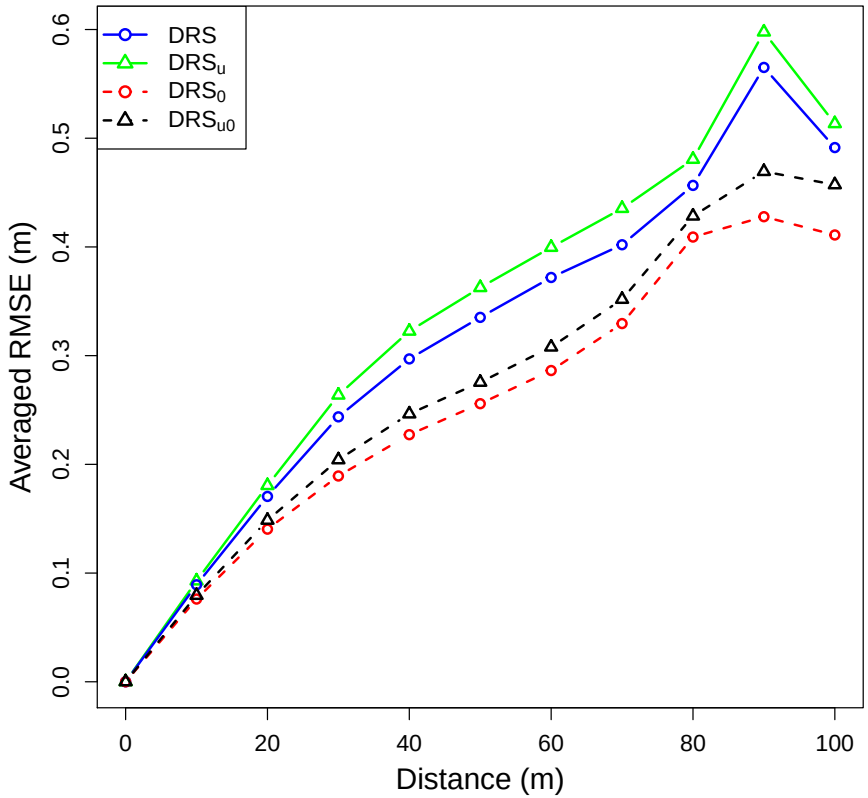

Figure: Averaged RMSE of DRS, DRS$_u$, DRS$_0$, and DRS$_{u0}$ at different distances. (a) US-101 dataset and (b) I-80 dataset.

Computational efficiency

- We conduct a time benchmark using simple linux unity for resource management (SLURM) computing resource on the high-performance computing cluster.
- The core processors are Intel® Xeon® CPU E5-2670 v2 (25M Cache, 2.50 GHz). We use one core for one simulation run.

Table: The mean and the standard deviation (in parenthesis) of modeling time in seconds for different trail sample sizes.

Dataset	Trail sample size				
	$\leq$50	51-100	101-150	151-200	201-250
US-101	0.0090 (0.0020)	0.0093 (0.0020)	0.0099 (0.0019)	0.0105 (0.0021)	– –
I-80	0.0090 (0.0021)	0.0095 (0.0021)	0.0101 (0.0021)	0.0106 (0.0021)	0.0107 (0.0023)

Computational efficiency

- We conduct a time benchmark using simple linux unity for resource management (SLURM) computing resource on the high-performance computing cluster.
- The core processors are Intel® Xeon® CPU E5-2670 v2 (25M Cache, 2.50 GHz). We use one core for one simulation run.

Table: The mean and the standard deviation (in parenthesis) of modeling time in seconds for different trail sample sizes.

Dataset	Trail sample size				
	$\leq$50	51-100	101-150	151-200	201-250
US-101	0.0090 (0.0020)	0.0093 (0.0020)	0.0099 (0.0019)	0.0105 (0.0021)	– –
I-80	0.0090 (0.0021)	0.0095 (0.0021)	0.0101 (0.0021)	0.0106 (0.0021)	0.0107 (0.0023)

Computational efficiency

- We conduct a time benchmark using simple linux unity for resource management (SLURM) computing resource on the high-performance computing cluster.
- The core processors are Intel® Xeon® CPU E5-2670 v2 (25M Cache, 2.50 GHz). We use one core for one simulation run.

Table: The mean and the standard deviation (in parenthesis) of modeling time in seconds for different trail sample sizes.

Dataset	Trail sample size				
	$\leq$50	51-100	101-150	151-200	201-250
US-101	0.0090 (0.0020)	0.0093 (0.0020)	0.0099 (0.0019)	0.0105 (0.0021)	– –
I-80	0.0090 (0.0021)	0.0095 (0.0021)	0.0101 (0.0021)	0.0106 (0.0021)	0.0107 (0.0023)

Outline

Conclusion

- This study presents a methodological framework for road geometry estimation.
- The proposed LMM approach, including newly developed trail compression and chopping mechanisms, facilitates accurate estimation for the shape of the road.
- The proposed methodology is applicable to vehicle following applications or to fuse with other sources such as vision lane markings to have a more accurate road shape estimation.
- The empirical results demonstrate that our proposed method can work reasonably well to estimate the highway road shape.
- The proposed trail compression and chopping mechanisms can greatly reduce the trail sample size as well as the modeling time of the LMM method.

Conclusion

- This study presents a methodological framework for road geometry estimation.
- The proposed LMM approach, including newly developed trail compression and chopping mechanisms, facilitates accurate estimation for the shape of the road.
- The proposed methodology is applicable to vehicle following applications or to fuse with other sources such as vision lane markings to have a more accurate road shape estimation.
- The empirical results demonstrate that our proposed method can work reasonably well to estimate the highway road shape.
- The proposed trail compression and chopping mechanisms can greatly reduce the trail sample size as well as the modeling time of the LMM method.

Conclusion

- This study presents a methodological framework for road geometry estimation.
- The proposed LMM approach, including newly developed trail compression and chopping mechanisms, facilitates accurate estimation for the shape of the road.
- The proposed methodology is applicable to vehicle following applications or to fuse with other sources such as vision lane markings to have a more accurate road shape estimation.
- The empirical results demonstrate that our proposed method can work reasonably well to estimate the highway road shape.
- The proposed trail compression and chopping mechanisms can greatly reduce the trail sample size as well as the modeling time of the LMM method.

Conclusion

- This study presents a methodological framework for road geometry estimation.
- The proposed LMM approach, including newly developed trail compression and chopping mechanisms, facilitates accurate estimation for the shape of the road.
- The proposed methodology is applicable to vehicle following applications or to fuse with other sources such as vision lane markings to have a more accurate road shape estimation.
- The empirical results demonstrate that our proposed method can work reasonably well to estimate the highway road shape.
- The proposed trail compression and chopping mechanisms can greatly reduce the trail sample size as well as the modeling time of the LMM method.

Conclusion

- This study presents a methodological framework for road geometry estimation.
- The proposed LMM approach, including newly developed trail compression and chopping mechanisms, facilitates accurate estimation for the shape of the road.
- The proposed methodology is applicable to vehicle following applications or to fuse with other sources such as vision lane markings to have a more accurate road shape estimation.
- The empirical results demonstrate that our proposed method can work reasonably well to estimate the highway road shape.
- The proposed trail compression and chopping mechanisms can greatly reduce the trail sample size as well as the modeling time of the LMM method.

Thank You!